Breakup and explosion of droplets of two immiscible fluids and emulsions

Antonov D.V., Piskunov M.V., Strizhak P.A.*

National Research Tomsk Polytechnic University,

30, Lenin Avenue, Tomsk, 643050, Russia

** Corresponding author. Tel.: +7 (3822) 701-777, ext. 1910*

E-mail: piskunovmv@tpu.ru. Website: http://hmtslab.tpu.ru.

Abstract

The explosive breakup of liquid, emulsion, and slurry droplets enables a several-fold increase of their evaporation surface area. This effect reduces the energy and time required for fuel heating, evaporation, and ignition. It also lowers anthropogenic emissions and provides fuller fuel burnout. However, the conditions and possible regimes of explosive breakup of liquid, slurry and emulsion droplets have yet to be found. Knowledge on such processes is necessary for improving the performance of fuel ignition and combustion as well as thermal and flame liquid treatment. Component mixing and storage may differ. The experiments in this research compare the explosive breakup of heated droplets of two immiscible fluids (e.g., water / flammable liquid) and water-in-diesel (W/D) emulsions stabilized by monoethanolamides of fatty acids. The experiments used the most widespread combustible liquids and fuels applied in the industry: kerosene, gasoline, diesel, petroleum oils, as well as petroleum. The most valuable findings are as follows: the experimentally established threshold conditions of droplet breakup, two regimes of droplet fragmentation, four outcomes of the parent droplet heating, as well as the number and size of the resulting fuel aerosol droplets. Another important experimental result consists in determining the maximum droplet heating times to explosive breakup corresponding to the equal proportions of water and flammable liquid (or fuel) in a droplet. If one of the components significantly exceeded the other one in proportion, the shortest heating time to droplet breakup was observed. The focus was on comparing the characteristics and parameters of droplets of W/D emulsions and droplets of two immiscible fluids. W/D emulsion droplets break up to form a fine aerosol, whereas two-component droplets show two breakup regimes: puffing and micro-explosion. The results obtained are important for the development of high-potential gas-vapor-droplet technologies to intensify the evaporation of additives and the ignition of fuel compositions.

Keywords: immiscible fluids; water-in-diesel emulsions; puffing; micro-explosion; fuel aerosol; Planar Laser Induced Fluorescence.

1. Introduction

Researchers of fuel technologies historically focus on a narrow but the most pressing scope of problems [1]. In particular, they are actively searching [1] for ways to minimize fuel consumption,

increase combustion dynamics, reduce anthropogenic emissions from fuel combustion, promote its complete burnout, improve the quality and reduce the cost of fuel preparation and spraying.

Current systems of flame and thermal water treatment unfortunately show rather low performance [2–4], because the liquid to be purified has to be supplied to the thermal purification chamber repeatedly. One cycle in the heating chamber is not enough for impurities to evaporate or burn out completely, and repeated cycles increase energy consumption and prolong the whole process.

In both fuel technologies and thermal treatment, a rational way to solve this problem could be by droplet breakup into smaller droplets sized several dozens or several hundreds of microns. However, experiments [5–7] show that such small droplets may be blown away from the thermal treatment chamber at low velocities (due to high velocities of heated flue gases or opposing air flow) or stick to the combustion chamber walls. Therefore, early disintegration of droplets before their supply to heating chambers may cause further technological complications and limitations. In this case, it is rational to start droplet breakup in combustion or thermal treatment chambers when heating is in progress. Colleagues from all over the world are making their attempts to develop the corresponding technologies. The most appealing technology in terms of stability, energy and time required is droplet boiling and explosive breakup to form fuel aerosol. So far, we can only single out experimental research (e.g., [8–15]) into explosive boiling of droplets of liquids, solutions, emulsions, and slurries followed by their disintegration to form aerosol.

Among the first researchers who paid attention to spraying and explosive breakup of boiling fuel droplets were the authors of researches [8–10]. According to their studies, these processes largely depend on molecular interactions as well as the amount and concentrations of vapor bubbles forming in droplets. In [8–10], they establish that water emulsion droplets rich in CO_2 need less overheating and shorter heating time to boil and break up, because dissolved CO_2 reduces the bubble nucleation energy. These results explain the reasons behind more rapid heating and boiling of water emulsion droplets. In [8–10], the explosive breakup of emulsion droplets occurred at high temperatures and with high concentration the oil product. Under these conditions, dissolved CO_2 plays a paramount role according to conclusions from researches [8–10]. Therefore, water emulsion droplets boiled and broke up after a short heating time followed by the formation of a large aerosol cloud with a CO_2 smell. Using a simplified mathematical model based on experiments from researches [8–10], we can predict how dissolved CO_2 will affect the heating and boiling of water emulsion droplets.

Papers on fuel aerosol burning in combustion chambers of motors and boilers have also become widely known (e.g., *Yin et al.* [11] and *Nau et al.* [12]). The breakup of fuel jets and films in airplane and automotive engines by an oxidizer flow is studied in [13]. Spontaneous disintegration of heterogeneous fuel droplets is the focus of researches [14, 15]. However, the scope of this research was limited to water emulsions and the methods only involved infrared recording. Based on the analysis of data from

researches [11–15], we can outline a significant change in the evaporation surface area and a decrease in the phase transformation time.

Tarlet et al. [14, 15] attempt to develop a numerical model simulating the breakup of fuel films by the air flow using experimental plots and the corresponding factors. They show an acceptable correlation between the experimental and calculated droplet volume and fuel film breakup characteristics when the fuel-air mixture is prepared for ignition. However, they did not apply the methods necessary to reliably measure the temperature fields of heterogeneous droplets and identify the threshold temperatures at the interface between droplet components where the explosive breakup occurs. Thus, the processes involved in droplet breakup remain understudied. It is important to apply combined measurement schemes including contact and non-contact methods of temperature gradient recording. The authors of researches [16,17] ascertained that water becomes less dense under heating, and surfactant molecules in it start to interact hydrophobically if their concentration is less than 0.1 wt.%. As a result, the amphiphilic molecules aggregate, further promoting droplet breakup into a large number of liquid fragments.

The authors of researches [18–21] attempt to apply such combined measurement schemes based on fast thermocouples and optic high-speed cross-correlation recording techniques: *Planar Laser Induced Fluorescence (PLIF)* [22–26], *Laser Induced Phosphorescence (LIP)* [27], *Particle Image Velocimetry (PIV)* [28], *Interferometric Particle Imaging (IPI)* and *Shadow Photography (SP)* [29], *etc*. As a result, studies [18–21] ascertained the threshold conditions of local two-phase droplet boiling (*water / solid inclusion* and *water / combustible liquid*) and the main attributes of these processes: heating time, surface transformation rate, as well as the number and size of droplets being formed.

The analysis of experimental results [18–21] helped the authors single out stages of heterogeneous droplet vaporization including evaporation from its free (external) surface, bubble boiling at the interfaces, growth of bubbles and increase in the droplet size with a decrease in the liquid film thickness around the inclusion, and explosive breakup (separation of a group of small droplets with vapor and air bubble in them). The authors also established that adding small (under 0.05 mm) nontransparent carbonaceous inclusions (mass fraction under 2 wt%) to water droplets reduces droplet lifetimes by 40–50 % as compared to droplets containing one nontransparent solid inclusion in the case of evaporation from a free surface. They showed how much a vapor layer around droplets (serving as an extra thermal insulation due to low thermal conductivity) affects the intensity of droplet evaporation. When a water droplet with a solid inclusion is heated in the air at a temperature of over 700 °C, the evaporation surface area may increase 3–15 times relative to the initial droplet surface area due to rapid liquid vaporization with its explosive breakup into small fragments.

Studies [18–21] established the integral characteristics of boiling, surface transformation, and overheating for droplets of water and water-based slurries when radiative heat flux from the external gaseous medium dominates the convective one. They determined the necessary and sufficient conditions for explosive breakup of boiling droplets of water slurries with a group of carbonaceous and soil additives

as well as rather slow consecutive evaporation with the droplet remaining intact. The authors developed the first simplified models of heat and mass transfer considering the explosive breakup of droplets when heated in high-temperature gaseous media [18–21]. Using the *PLIF* technique [20, 21], they plotted calibration curves showing the correlation between the fluorescence of liquid fuel and its temperature. Such experiments have yet to be conducted with prepared emulsions, solutions, and slurries. The scientific community is still searching for methods to control the explosive breakup of droplets of fuels, combustible liquids, two immiscible fluids, solutions, emulsions, or slurries. It is important to develop physical and mathematical models to reliably forecast the outcomes of droplet breakup due to local overheating and boiling, possible regimes of these processes, differences of various mixing schemes, etc. This is only possible with reliable experimental database of characteristics and conditions for these effects.

In contrast to early studies [20, 30-32], this research focuses on a comparison of the breakup characteristics and outcomes for the two-component droplets of the immiscible fluids and the emulsion droplets. Such a comparison has not yet been performed. Research [20] considered the revealed regimes and lifetimes of the emulsion fuel droplets. In addition, this study includes the conclusion that the experimental data on characteristics and conditions for the intensive evaporation and boiling of the oil–water drops show that in future it is necessary to carry out investigations with different impurities. In study [30], the optical method PLIF was applied for the first time to explore temperature fields in two-component droplets. It is established that the boiling droplets of water emulsions may break up in one of the three modes, which differ in duration and number of the emerging small droplets. The ranges of the variation of the heating temperature and additive concentration corresponding to each of the three modes were determined: the first one (temperature over 200°C, concentration γ = 7–33%), the second one (temperature over 280°C, concentration γ = 33–66%), and the third one (temperature over 400°C, concentration γ > 66%). The area of the liquid evaporation surface may increase several fold during the breakup of water slurry droplets. The number of droplets forming in the third mode is dozens of times larger than in the first mode. Research [31] experimentally studied the processes of explosive disintegration of heated fuel droplets with variations of the added water volume. In addition, the effect of the laser and water film on the microexplosion process were examined. Study [32] reported the effect of different holders on the explosive breakup process. During the analysis of the heating times of the two-component droplets until breakup, we discovered that the disintegration times of two-component droplets are minimum when holders with a low thermal diffusivity are used (a<$10 \cdot 10^{-6}$ m^2/s), and maximum when thermal diffusivity is high (a>$80 \cdot 10^{-6}$ m^2/s). Thus, we demonstrated that the effect of experimental methods, materials, properties, and concentrations of droplet components on the microexplosion characteristics was explored in sufficient detail. However, a comparison of the threshold (critical, necessary and sufficient) conditions and breakup characteristics for the emulsion and two-component

(from the immiscible fluids) droplets under the strong heating has not yet been performed. This is the scientific novelty of the study.

The purpose of this work is to establish experimentally the conditions and characteristics for the explosive breakup of heated droplets of two immiscible fluids and W/D emulsions.

2. Experimental technique

2.1. Materials

The substances used in the experiments are typical of fuel technologies as well as thermal and flame water treatment (Table 1): kerosene, gasoline, diesel, oil, and petroleum. Table 1 contains the generalized information from researches [1, 8–15, 20, 33, 34] for further analysis of how experimental results may change if liquid flammable components are used from various regions of the world.

Table 1. Main properties of liquid flammable components and water (based on data from researches [1, 8–15, 20, 33, 34]) at 20°C.

Sample	ρ, kg/m^3	μ, Pa·s	σ, 10^{-3} N/m	T_f, °C	T_i, °C	Q_c, MJ/kg	T_b, °C	Q_v, MJ/kg
Petroleum oil	877	0.0019	28.5	148	169	44.98	320–330	0.167–0.209
Kerosene	885	0.0026	24.2	30–60	140	43.8	180	0.261
Gasoline	750	0.0022	23.7	40–49	180	44.2	147–220	0.235
Diesel	820	0.0029	27.6	40–85	200	42.4	240–347	0.210
Petroleum	885	0.0021	26.1	55–120	300	44.31	105–160	0.210
Water	997	0.0014	72.6	–	–	–	100	2.26

W/D emulsions were stabilized using a nonionic emulsifier of fatty acid monoethanolamides with an HLB value (hydrophilic-lipophilic balance) of 2. Fatty acid monoethanolamides–tall oil fatty acids and monoethanolamine condensation products–are classified as alkylolamides. This stabilizer was obtained, as described in [35], by direct vacuum amination of tall oil distillate by monoethanolamine at 150–160 °C (acid value 11.5 mg KOH/g). We developed this nonionic emulsifier (3 wt%) to provide greater stability of W/D emulsions [36] as compared to W/D emulsions stabilized by commercial analogs, for example *SPAN-80* and *TWEEN 85* [37].

The experiments were conducted under identical conditions using two-component droplets and tailored W/D emulsions with surfactants. Below you will find comments on how the structure and composition of droplets differed in these cases.

2.2. Two-component droplets

Fig. 1 shows a simplified scheme of obtaining a two-component droplet (by electronic dispenser *Finnpipette Novus* with a pitch variation of 0.1 μl). The initial volume V_d of a two-component ranged

from 10 to 25 µl. This corresponded to the range of radius variation R_d=1.3–1.8 mm. Smaller two-component droplets were difficult to obtain, because an electronic dispenser cannot produce droplets smaller than 5 µl. Droplets of larger volume fell off the holder even before being placed into the heating chamber. In the experiments in [20], two schemes were used for obtaining two-component droplets. The first one involved suspending a water droplet on a holder. Then one more *Finnpipette Novus* dispenser was used to insert a droplet of the combustible component. As the high-speed video recording shows, a combustible additive usually enveloped a water droplet, thus creating a 0.05–0.5 mm film on its surface. In most cases, water was located at the top of the droplet, touching the holder, while the flammable additive gravitated to the bottom. The second method, on the contrary, implied placing a droplet of flammable liquid on the holder and adding water. In this scheme, a combustible additive gathered at the top of the droplet and water concentrated at the bottom. The surface tension of the liquid flammable component is much lower than that of water. So, the maximum effect of micro-explosive breakup can be achieved if water is used in the center and the liquid flammable component serves as an envelope. In accordance with experimental results from research [20], we chose the first recording scheme for this study. A steel *X6CrNiMoTi 17-12-2* hollow metal rod 0.3 mm in inner diameter and 0.6 mm in outer diameters served as a droplet holder for both two-component and W/D emulsions. As compared to other materials (ceramics, phosphorus, iron, nichrome, etc.) as well as droplet fixation schemes on the holder, a hollow metal rod made the least influence on the heating of the droplets under study. The corresponding evaluations were made in [38] by comparing the experimental and theoretical research findings.

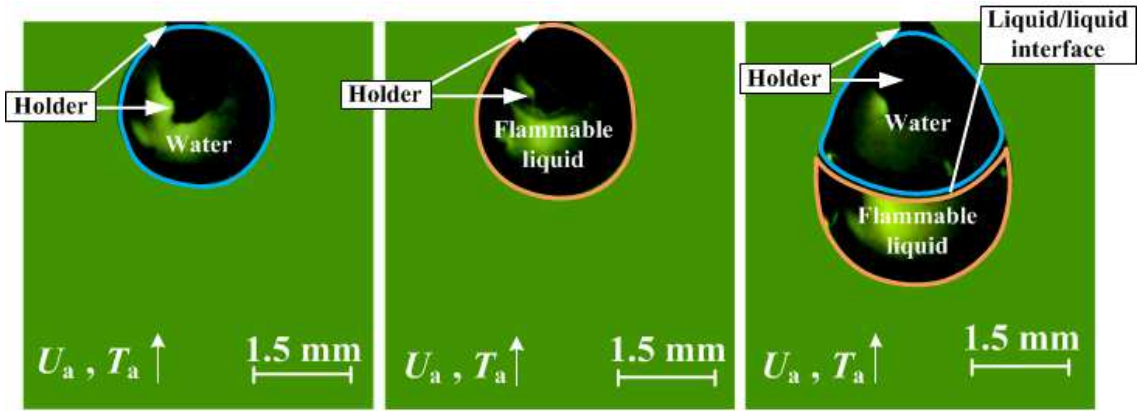

a *b* *c*

Fig. 1. Appearance of initial droplets of water (*a*) and combustible component (*b*), as well as a typical two-component droplet with an indicated liquid / liquid interface (*c*).

As in the experiments from researches [19–21], the component concentration in a two-component droplet could only be varied in limited increments due to the corresponding limitations as to the volume increments of droplets produced by Finnpipette Novus dispensers. Water fraction was varied from 3 vol% to 97 vol% to embrace a wide range of technologies mentioned in the *Introduction Section*.

2.3. Water-in-diesel emulsion

For W/D emulsions we used summer diesel fuel DT-L-K5 according to the RF state standard GOST 32511-2013, with a density of 0.832 g/cm^3 (at 18 °C) and kinematic viscosity of 2.065 cSt (at 40 °C) as well as distilled water with the specific conductivity of no more than 5 µS/cm. The surfactant (3 wt%) used to stabilize the emulsion was described in detail in Section 2.1.

Emulsions were produced using a high-speed *GJ-3S* mixer (*Qingdao Chuang Meng Instrument Co., Ltd., China*). An emulsifier sample was dissolved in diesel fuel of a dispensed volume. While mixing the resulting solution at a rate of 11,000 rpm, we gradually added the required volume of distilled water to it and then mixed it for 7 minutes under the same conditions. The resulting emulsion was degassed under vacuum produced by an aspirator for at least 20 minutes. Fig. 2 shows frames of a typical W/D emulsion droplet.

The image in Fig. 2b was obtained by *Laser Scanning Confocal Microscopy (LSCM)* using a *ZEISS LSM 780 NLO* microscope in the *T-PMT* mode (transmitted light detector) with a laser line of 405 nm. Fig. 2*c* presents the internal-phase droplet dimensions in the W/D emulsion sample under study. The droplet dimensions were calculated using the J 1.51 s application (*Wayne Rasband, National Institutes of Health*). The most frequent water droplet diameter in the emulsion was 0.8–0.9 µm. The average droplet diameter was 1.2 µm. The average internal-phase droplet dimensions obtained are in good agreement with the similar parameter in the previous research of micro-explosions in W/D emulsion droplets and overall in water-in-oil (W/O) emulsion droplets [39, 40]. The W/O emulsions with such average dimensions of internal-phase droplets are considered finely divided [39] but not the most effective in terms of droplet breakup outcomes induced by a micro-explosion [40].

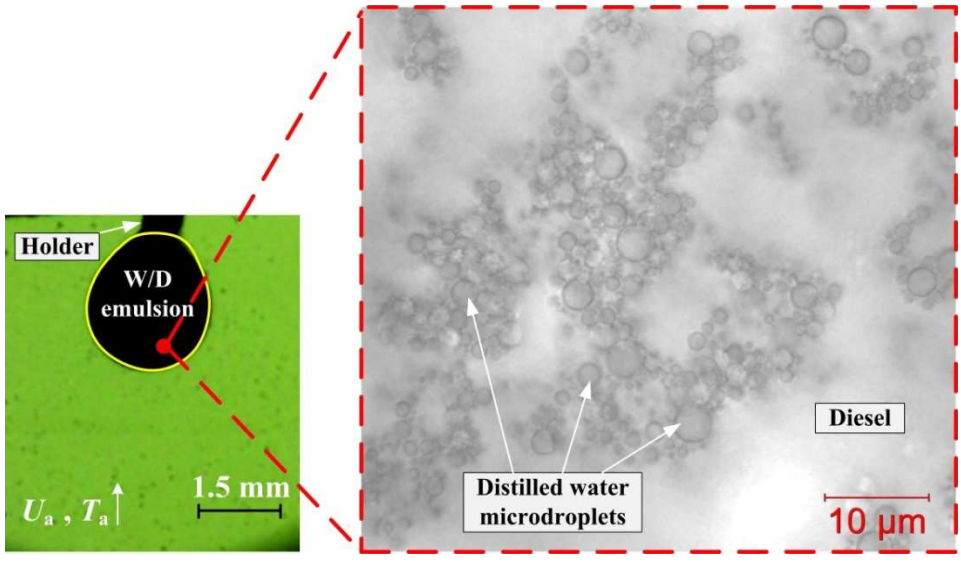

a *b*

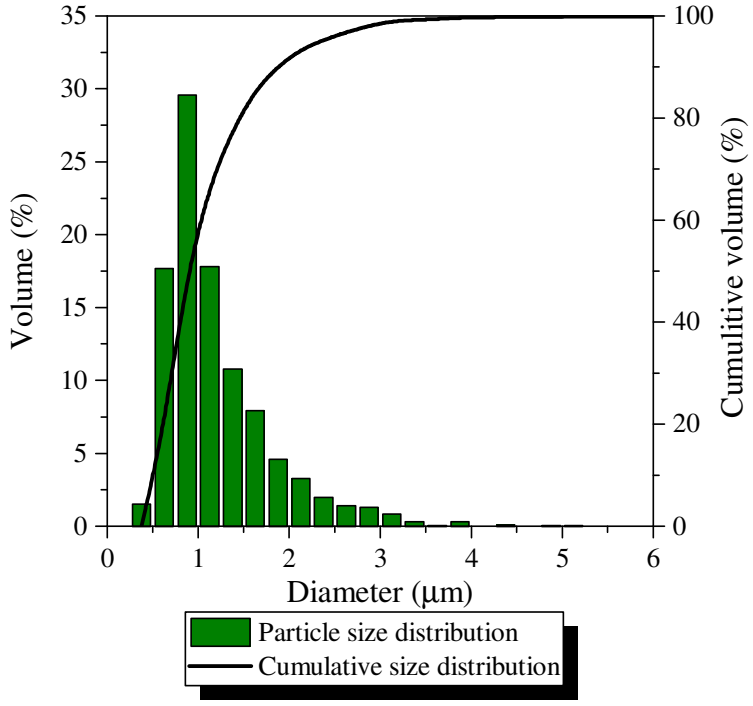

c

Fig. 2. Droplet of typical W/D emulsion (*a*); LSCM images of the emulsion by a 405-nm laser (30 vol% water phase, 3 wt% emulsifier) (*b*); Size distribution of water droplets in the tested W/D emulsion (*c*); micrograph of the emulsion was obtained using the equipment from Tomsk regional common use center.

2.4. Planar Laser Induced Fluorescence measurement

In order to measure the temperature of two-component droplets using the PLIF technique like in experiments from researches [20, 41], we used the following hardware and software (Fig. 3): a cross-correlation camera, a macro lens, a light filter blocking excessive laser light, a fluorescent dye, a dual pulsed laser, a lens for generating a light sheet with an adjustable opening angle, as well as a personal computer with the *Actual Flow* software and *PLIF Kit* module. As in [20], we chose *Rhodamine B* as a fluorophore, because it does not dissolve easily in typical oil products and flammable liquids, unlike, for instance, *Pyrromethene 597-C8* [20]. This allowed us to record the temperature distribution near the *water (with Rhodamine B) / flammable liquid* interface. Special aspects and limitations of PLIF measurement of liquid droplet temperature as compared to numerical simulation are described in [38].

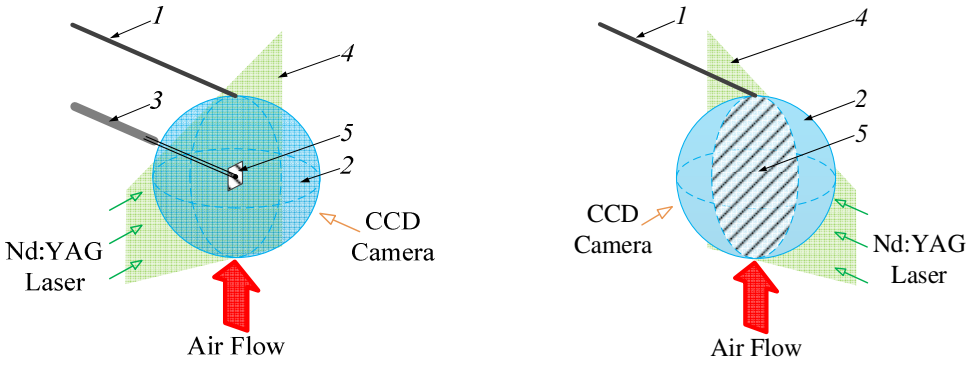

a *b*

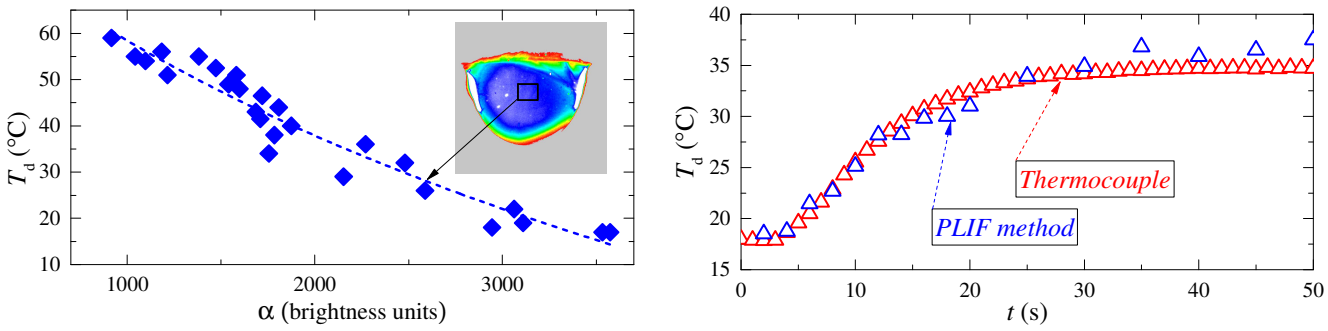

c *d*

Fig. 3. PLIF scheme during system calibration *(a)* and during the experiment *(b)*: *1* – holder; *2* – droplet; *3* – fast-response thermocouple; *4* – light sheet; *5* – video recording area; experimental calibration curve (*c*) and the comparison of temperatures in the droplet center (at V_d≈10 µl, R_d≈1.53 mm, U_a≈3 m/s, T_a≈100 °C) obtained by PLIF technique and a small thermocouple (*d*) [41].

For the experiment, we used the dual pulsed laser with a frequency of 4–10 Hz to cut the droplet along the axis of symmetry. The pulse frequency is adjusted depending on the experimental conditions. *CCD* images of the droplet were processed with the *ActualFlow* software. The light sheet was 100 µm thick to ensure the minimum constant density of laser radiation in the measurement area.

The experiments were performed in two stages (Fig. 3). *At the first one,* we calibrated the measurement system using a fast thermocouple and a water droplet without any additives. *The second stage* involved recording the temperature field of an evaporating two-component droplet while varying the temperature of the air flow. The main procedures performed on water droplets are described in detail in [20, 41]. Below you can see a brief description taking into account the specific aspects of objects under study.

The first stage involved generating a set of *CCD* images at a constant water temperature throughout the measurement area. We performed the measurements for no less than 20–30 air temperature values in the range of 20 °C to 550 °C in order to obtain a calibration curve of reasonable accuracy. Temperature deviations in the measurement area did not exceed the measurement errors of thermocouples used for calibration under the same heating conditions. The experimentally obtained calibration curve showed the dependence between the temperature and Rhodamine B fluorescence expressed in units of brightness. We used a fast-response thermocouple (platinum-platinum-rhodium, 0.05 mm junction diameter, 0.1 s time lag) for calibration with its junction placed in the center of mass of a water droplet. The droplet with a thermocouple inside was introduced into the quartz-glass cylinder with the heated air. The droplet temperature field $T_d(R_d, t)$ was adjusted by varying the air temperature T_a. The thermocouple junction was moved in the droplet by a motorized manipulator to record the water temperature T_d at different points of the heated droplet section. This way we obtained the T_d=$f(T_a)$ functions. At least 100 images were generated for each value of the air temperature T_a following the PLIF developers' recommendations. The resulting images with the corresponding fluorescence fields

were averaged, and then noise excluded from each averaged image. The calibration curve was plotted using the image processing by *PLIF Calibration* and thermocouple measurements. For higher accuracy, a small droplet section area (0.5×0.5 mm) was selected near the thermocouple junction. The thermocouple also recorded 100 T_d values in the identical sections during the corresponding heating times.

At the second stage, we recorded the heating, evaporation, and explosion of two-component droplets with the constant operating parameters of the laser and camera and without changing the measurement area, background illumination, and equipment layout. After the experiments, *CCD* images were processed with the *ActualFlow* software, using *PLIF Reconstruction* based on the calibration curve from the first stage. Temperature fields were determined in the droplet sections produced by the light sheet.

For the identical initial conditions, we conducted three to five series of experiments. Each series consisted of 100–1,000 images of the droplet when its heating and evaporation was in progress (throughout its lifetime). The imaging process began at the moment when a two-component droplet was placed in the center of the quartz-glass cylinder and finished when the droplet evaporated completely.

Fig. 4 presents the examples of the temperature fields of the heated two-component water-petroleum droplets at different petroleum concentrations (3 vol% and 5 vol%). The temperature fields are measured by using the PLIF method for water. For the combustible part (petroleum) of droplets, such fields have not been measured because there is no corresponding dye. The temperature fields enabled to state that the temperature inside the droplet before breakup exceeded the boiling point. In the case of a lower concentration of water in a droplet, a larger volume of this component heated up to temperatures close to the boiling point. With an increase of the water concentration, only local regions were able to heat up to such high temperature. However, this was enough for the nucleation and growth of the bubbles filled with water vapors, the collapse of which resulted in the explosive droplet breakup in spite of the presence of the subcooled layers.

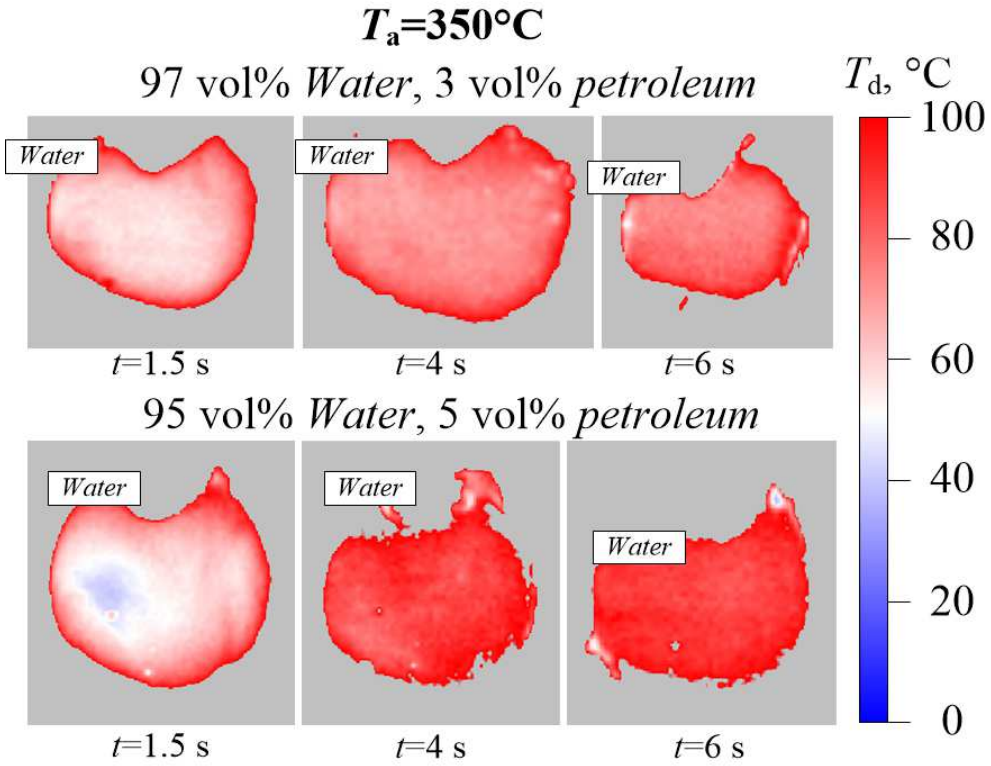

Fig. 4. Temperature fields measured by the PLIF method during the overheat of the two-component water-petroleum droplets at different water concentrations, namely 3 vol% and 5 vol% for flammable liquid.

2.5. Experimental procedure of research into the outcomes of droplet collision

Using a high-speed video camera Phantom Miro M310 with a frame rate 3260 fps at a resolution 1280x800 px, we recorded the heating and disintegration of heterogeneous droplets. We then processed the video recordings using the *Tema Automotive* and *ActualFlow* software with the continuous tracking of moving objects. In the course of processing, we determined the initial droplet size R_d and the total evaporation surface area S (Fig. 5).

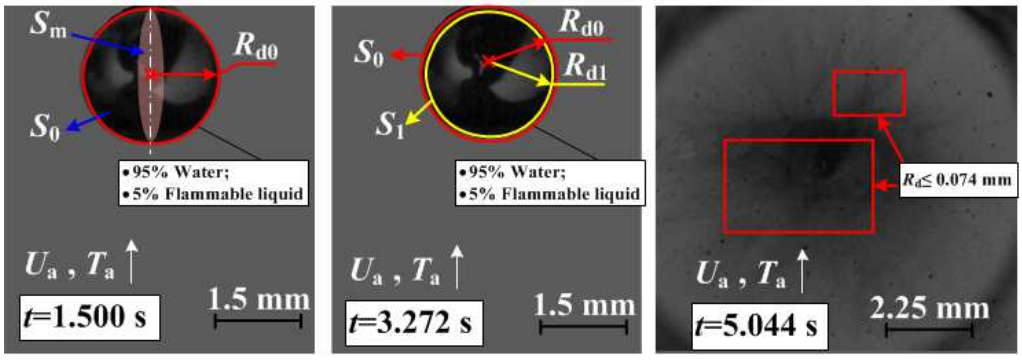

Fig. 5. Scheme of recording the disintegration of a heated droplet of two immiscible fluids and aerosol generation.

The video recordings were processed in two stages. At first, we tracked the changes in the frontal cross-sectional area S_m of an evaporating and deforming droplet until it broke up (Fig. 5). Using the

Airbag and *Advanced Airbag* tracking algorithms, we measured the changes in the shape of an evaporating droplet. Then we calculated the frontal cross-sectional area of a droplet and plotted the curves $S_m(t)$. To simplify the calculation process, we assumed the droplet to be spherical and its frontal cross-sectional area to be a circle. The average droplet radius R_d was calculated using the formula $R_d=(S_m/\pi)^{0.5}$. These measurements could be done at any moment during the video recording. The errors of the R_d calculation were under 2.5 %. After that, using the formula $S=4\pi R_d^2$, we calculated the total area of the droplet evaporation surface.

At the second stage, we used the *Actual Flow software* to analyze the videos after a heterogeneous droplet broke up into separate smaller fragments, usually forming a polydisperse aerosol. We carried out the digital analysis of the shadow image to determine the location, boundaries and dimensions of isolated droplets. *Median*, *Low Pass* and *Average* software filters were used to screen off the noises. *Laplace Edge Detection* determined the boundaries of droplet surface. To determine the droplet dimensions, we applied the *Bubble Identification* algorithm used for *Shadow Photography* [32]. The error of the R_d calculation did not exceed 3 %.

This way we obtained the droplet size distributions. All the droplets were classified into *m* groups. For each group, we determined the number of droplets *n* and the average droplet size R_{dn} in a group. The liquid evaporation surface for the droplets of each group was calculated by the formula $S_n=n\cdot 4\pi R_{dn}^2$. At the final step, we calculated the total evaporation surface area: $S=S_{n(1)}+S_{n(2)}+\ldots+S_{n(m)}$.

2.6. Droplet heating

The authors of research [41] discuss typical schemes of droplet heating to study the patterns of radiative, convective, and conductive heating. They show that the schemes with convective and radiative heating bring laboratory experiments closer to numerous real-life applications. Moreover, convective heating throughout the temperature range [41] provided a greater heat flow. Therefore, in this study we performed the main water droplet heating experiments in a heated air flow according to the scheme described in [41]. The used heating system is *Leister CH 6060* hot-air blower (air velocity of 0.5–6 m/s) and *Leister LE 5000 HT* air heater (temperature range of 20–1000 °C), generating the necessary parameters of the flow of high-temperature gases (velocity U_a and temperature T_a). Additional experiments involved heating two-component droplets and emulsion droplets in a muffle furnace. The experimental procedure in this case was generally similar to the experiments with convective heating, but the used heating system was the muffle furnace: maximum temperature of 1200 °C, chamber volume of 0.004 m^3, and the permissible deviation of ±1 °C.

2.7. Research parameters and accuracy

Table 2 lists the parameters recorded in the experiments as well as systematic errors of the measurement tools.

Table 2. Main registered parameters and tolerances.

Physical magnitude	Measurement tool / technique	Systematic errors
air temperature (T_a)	Temperature meter (IT-8)	± (0.2+0.001T)
air flow velocity (U_a)	Particle Image Velocimetry (PIV)	± 2%
droplet volume (V_d)	Finnpipette Novus dispensers	±0.05 µl
droplet radius (R_d)	High-speed cameras Phantom Miro M310 and Photron Fastcam SA1, Tema Automotive software	≤ 4%
temperature inside the droplet (T_d)	Planar Laser Induced Fluorescence (PLIF)	±1.5–2 °C
droplet heating and evaporation time while the droplet integrity is maintained (τ_h) droplet breakup time (τ)	High-speed cameras Phantom Miro M310, Photron Fastcam SA1, and Phantom V 411, Tema Automotive software	≤ 4%

We carried out the preliminary tests estimating the differences in temperature fields during the 2D and 3D measurements. The utilization of the second camera and laser enabled to measure temperatures in a droplet more precisely; a typical error was 0.17–0.4 °C [42]. The 3D measurement of a number and sizes of the emerging liquid fragments allowed us to refine data obtained during the 2D measurement. The maximum divergence between the results of the 2D and 3D measurements in terms of the ratios of the evaporation surface areas before and after the breakup (S/S_0) did not exceed 15%.

3. Results and discussion

3.1. Breakup modes

In the course of experimental research, we have identified four possible outcomes of two-component droplet heating (Fig. 6). Two of them are characterized by well-known droplet breakup modes [39–41, 43]: puffing (droplet fragmentation as in Fig. 6*b,c*; droplet destruction processes in these figures differ in the number and size of liquid fragments generated in the course of dispersion) and micro-explosion (complete destruction of the parent droplet as in Fig. 6*d*). Each of these outcomes had a number of special aspects. In outcome 1, for instance, a droplet rapidly heated and boiled but bubbles appeared locally rather than throughout the droplet. Therefore, at some point, due to the gas filling the droplet, it broke away from the rod (Fig. 6*a*). In outcome 2, bubbles emerged almost throughout the droplet. Bubble

destruction was accompanied by puffing (Fig. 6*b*). With an increase in the gas flow temperature or flammable liquid concentration, we could observe outcome 3 (Fig. 6*c*) and outcome 4 (Fig. 6*d*). In the latter two cases, the vaporization in the droplet was so intense that bubbles appeared throughout the droplet. However, in the case of outcome 3, a large number of droplets broke away in fractions (after 2–4 explosions, the droplet was destroyed). In outcome 4, the droplet surface did not undergo any changes at the onset of the heating process but then we registered a loud popping sound characterized by instantaneous droplet breakup. A finely divided aerosol was formed with clearly detectable vapors. The latter could be observed on camera (by a visible mist – smog) and detected by the smell of the flammable component vapors and carbon dioxide.

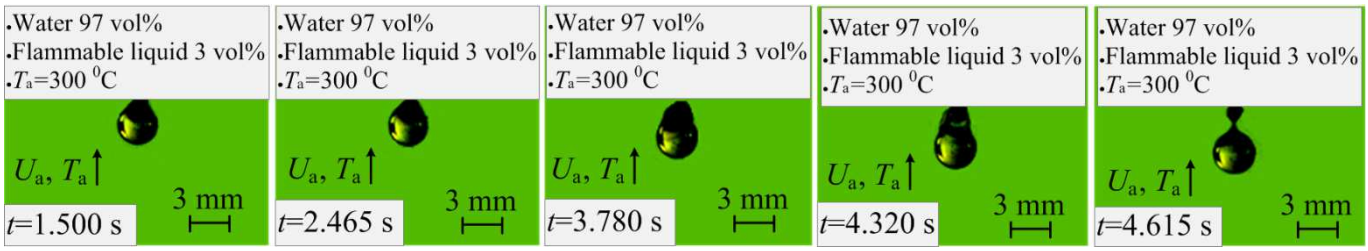

a

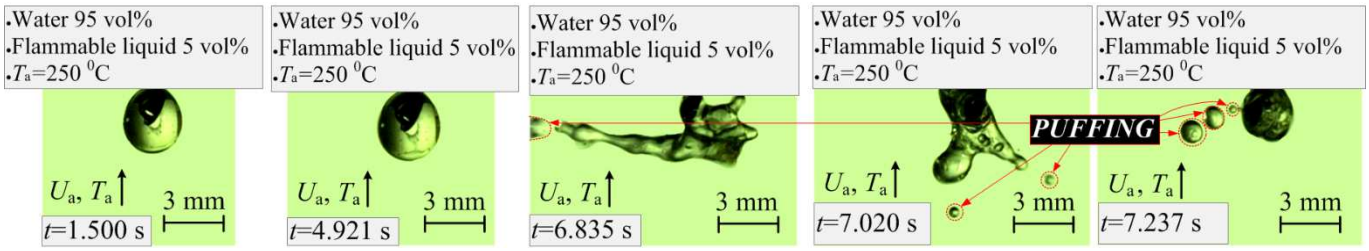

b

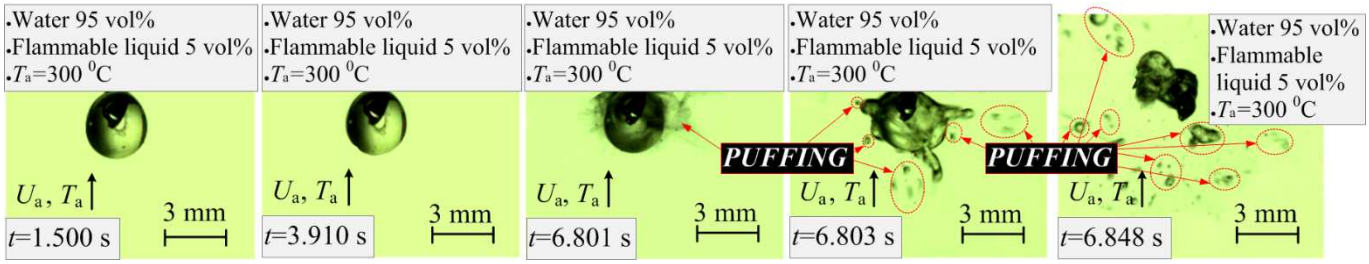

c

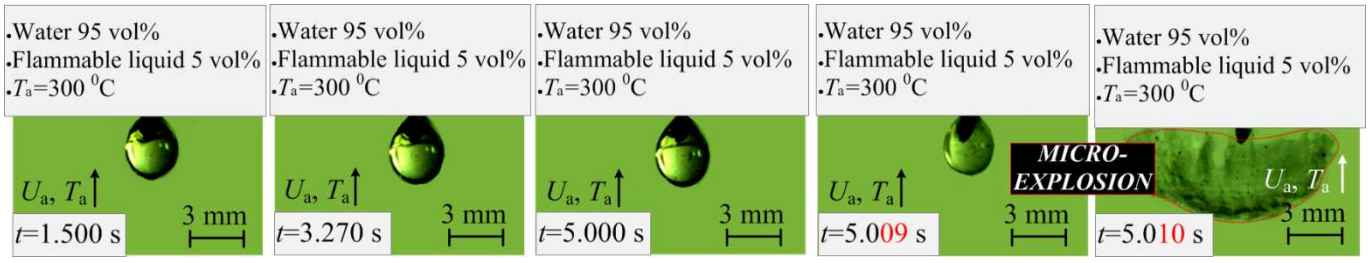

d

Fig. 6. Frames of the experiment showing four outcomes of two-component droplet heating: *a* – breakaway from the holder (outcome 1), *b* – dispersion of large fragments without disintegration (outcome 2), *c* – dispersion of polydisperse fragments with disintegration (outcome 3), *d* – explosive breakup (aerosol generation) (outcome 4).

Apart from experiments with two-component droplets, we experimentally studied emulsions with different flammable component concentrations (30 vol%, 50 vol%, 70 vol%). In these experiments, we identified two types of W/D emulsion behavior (Fig. 7): evaporation and dispersion. Droplet micro-explosion was not observed in any of the experiments, most likely because the explosive breakup of an emulsion droplet depends on the intensity of the local energy supply [41]. The local overheating of a droplet launches a chain [43] of "swollen" vapor bubbles collapsing throughout the droplet through the destruction of one bubble, *i.e.*, if there is a directed impact. In the experiments with emulsion droplets on a holder, we did record rapid heating but it was more uniformly distributed along the droplet surface. This energy supply mode is better at triggering the rapid evaporation from the free liquid surface. At the surface of a W/D emulsion is mostly diesel, and it starts evaporating at the onset of heating. This is confirmed by the video recording, in which a matte-white droplet turns transparent. This means that only water remains in the droplet and it is not going to break up, since there are no potential vaporization centers or surfaces. By the time the vapor bubbles begin exploding (due to water vaporization), the diesel concentration in a droplet plummets, thus reducing the chance of micro-explosion.

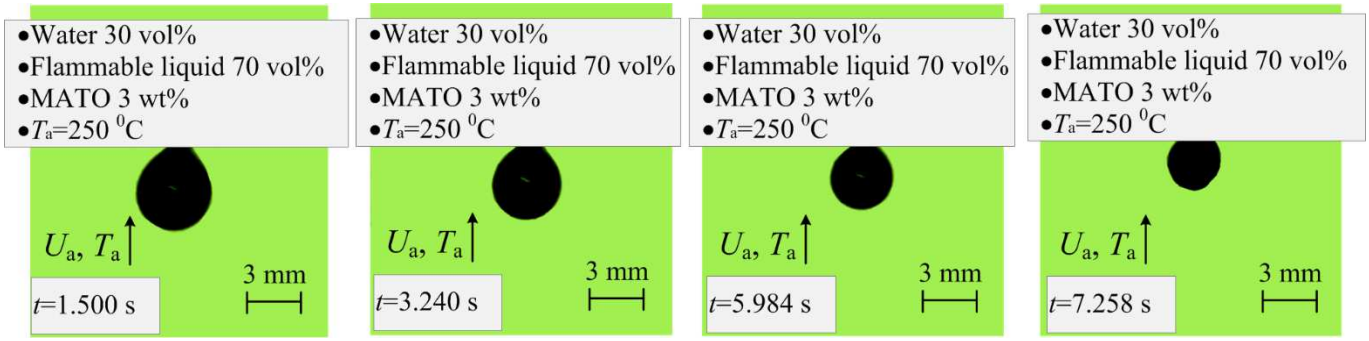

a

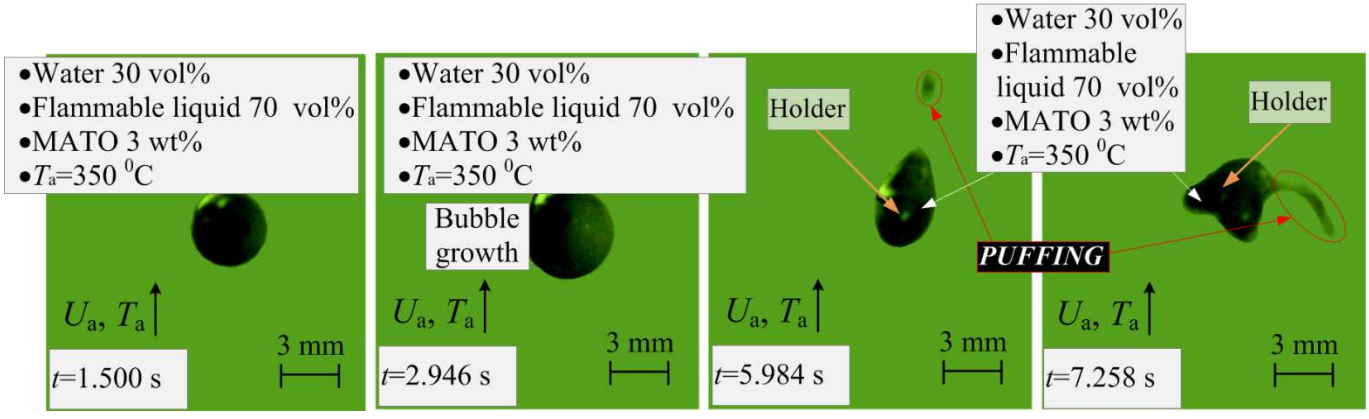

b

Fig. 7. Frames of experiment with two behaviors of W/D emulsions: evaporation *(a)* and dispersion *(b)*.

Dispersion of an emulsion droplet on a holder results from the heating of deep droplet layers but only at higher heating temperatures T_a. When an emulsion droplet is heated on a holder, vapor bubbles do not emerge throughout the droplet but only in some of its areas (anywhere but on the free surface). During

the destruction of a combined bubble (after coagulation of a group of bubbles), we can observe the dispersion behavior with quite large separated liquid fragments (Fig. 7*b*).

3.2. Threshold conditions of droplet breakup

Fig. 8 outlines temperature ranges for each of the four outcomes of two-component droplet heating, evaporation, and breakup (in accordance with video frames in Figs. 6, 7). Transient areas between the corresponding outcomes are shaded. In these areas, we observed two outcomes with different repeatability.

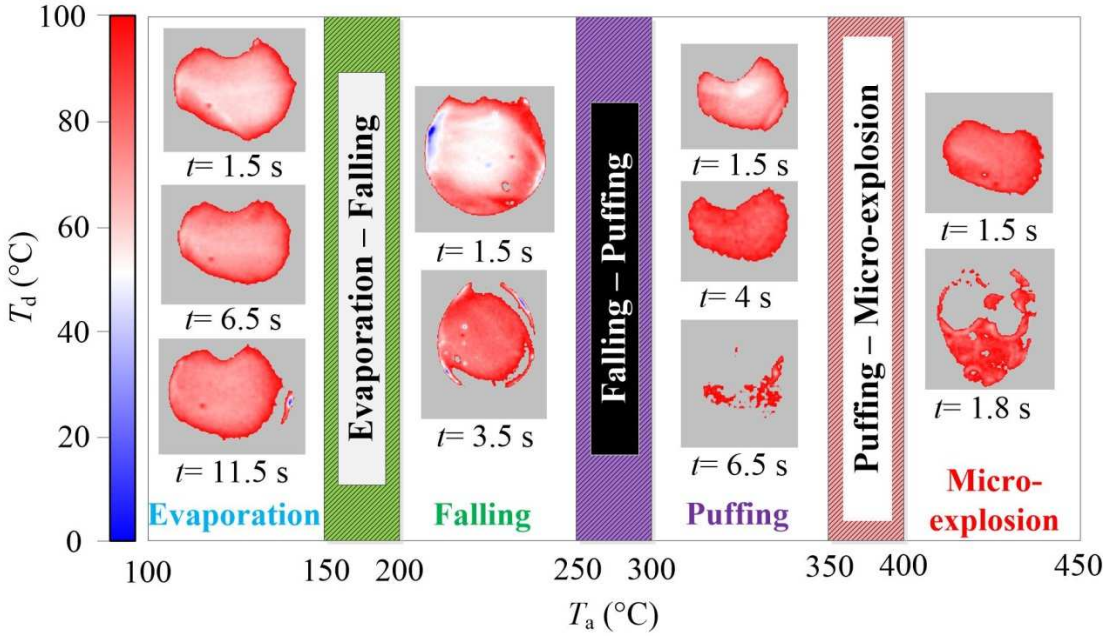

Fig. 8. Temperature ranges with different breakup behaviors of two-component droplets (95 vol% water, 5 vol% kerosene, V_d=15 µl, U_a=2 m/s) and typical temperature fields T_d of droplets.

By analyzing the droplet temperature fields obtained by *PLIF*, we ascertained the main physical mechanism of droplet breakup. It is based on the following patterns. Before the droplet breakup, water reached its boiling temperature, *i.e.*, 100 °C, at the *water / kerosene* interface. At the *fuel / water* interface, the temperature could reach 110–120 °C. This result illustrates how a vapor buffer layer is formed between the flammable and non-flammable liquids in this area. As can be clearly seen in Fig. 8, the heating of the whole water droplet up to such high temperatures does not guarantee the conditions for stable breakup. A droplet may reach 80–90 °C throughout its volume and gradually evaporate without disintegrating (*i.e.*, its integrity is maintained). The local overheating of two-component droplets leads to a chain activation of low-temperature centers of pressure pulse generation [43]. It was the main reason behind the destruction of *liquid / liquid* interfaces and explosive breakup of droplets. The breakup is accompanied by sonic and visual effects (popping sound and fragmentation) and yields finely divided aerosol and vapor mist.

The dye–fluorophore–added to the droplet did not dissolve in the flammable liquids under study (Table 1) [41]. Therefore, the PLIF technique could not be used to measure the temperature in the zones of two-component droplets filled with a flammable liquid. The temperature field of water was measured instead [41]. This differentiation made it possible to ascertain the heating mechanism of a two-component droplet. It is based on a more rapid heating of the liquid flammable phase and its evaporation due to lower heat of vaporization as compared to water. This became the reason why water was overheated at the *fuel / water* interface. In such areas, we detected zones filled with vapor bubbles. They were moving at speed in the droplets, forming convective currents. In some experiments, bubbles coagulated to form a single cavity in a droplet or rapidly left the free surface of the latter with liquid fragments breaking away as well. The greater the heat flux supplied to the droplet surface, the more intense the dispersion of local areas of two-component droplets (Fig. 8).

Unfortunately, while we do not have at hand a dye for the liquid combustible component. Therefore, we cannot measure the oil or diesel temperatures. At this time, there is a dye for kerosene, namely Solvent green 5. However, we have performed the experiments using the fast-response thermocouples measuring temperatures of the combustible and non-combustible components. The experimental results show that the combustible component heats up to a higher temperature. This is due to the combustible component has lower vaporization and specific heat, as well as high thermal diffusivity, emissivity, and absorptivity. Study [32] demonstrated temperature distributions calculated in the two-component droplets. These results illustrate the adequacy of the formulated conclusions in this research.

3.3. Quantitative estimates of the droplet breakup outcomes

Fig. 9 shows how much the total evaporation surface area may increase, when a finely divided aerosol is produced by an explosive breakup of two-component droplets with a volume of 15 μl, as an example. In this case, the initial evaporation surface area S_0 of the droplets was approximately 29.4 mm^2. The calculation made use of the formula for the area of a sphere $S_0=4\pi R_{d0}^2$, $R_{d0}\approx1.53$ mm, $V_d=15$ μl. The trends are similar for different component compositions (Fig. 9). The greater the difference between the relative concentrations (fractions) of liquids in a droplet, the greater the effect of explosive droplet breakup. Mixing liquids in equal proportions appeared to be ineffective. The more liquid flammable component and the less water, the more intense the droplet disintegration: the heating time before breakup was shorter and the number of droplets it formed was nonlinearly greater. The liquid flammable component is heated and the droplet is rapidly filled with bubbles of flammable gases and water vapors, which coagulated to form a vapor-gas cavity in the droplet. The droplet enlarged dramatically and the flammable liquid film became thinner. As a result, when the film reached threshold thickness values, it broke down to form a fine aerosol. The escaping gases and vapors formed smog in the high-speed recording area.

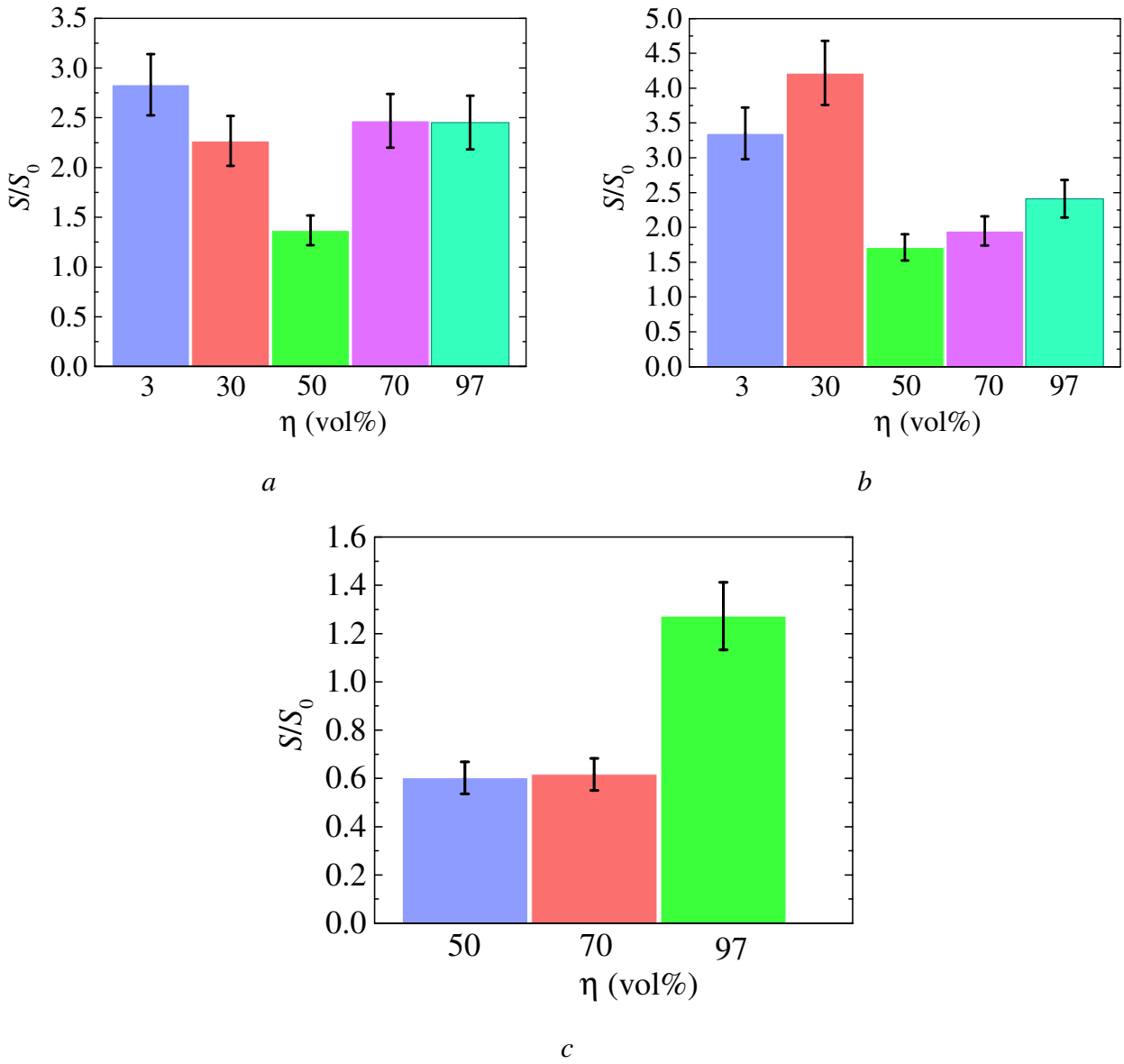

Fig. 9. Relative total evaporation surface area of a droplet after its disintegration at T_a=350 °C: (*a*) water and oil; (*b*) water and diesel fuel; (*c*) water and solvent; V_d=15 μl.

When comparing the heating and breakup characteristics of two immiscible fluids, we ascertained that the lower the boiling, flash, and ignition temperature of the flammable components (Table 1), the more rapidly the area S increases. This is conditioned by high mass vaporization rates of liquid fuel components [1, 33, 34]. At the same time, all the liquids are characterized by the exponential temperature dependence of vaporization rates [1]. Therefore, the droplet is filled with a large amount of flammable vapors and gases that have rather high temperature as compared to water. Water is heated very slowly due to its high heat capacity and high energy consumption for endothermic phase transformation.

Fig. 10 presents the results of the 2D and 3D recording of the explosive breakup outcomes of the two-component droplets during the strong heating. Among of them are the ratio between evaporation surface areas before and after breakup versus the oil concentration (Fig. 10*a*) and the size distribution of child-droplets (Fig. 10*b*). The comparison analysis of the results allowed the conclusion about the

reasonability and sufficiency of the 2D recording utilization to explore the breakup outcomes of the two-component droplets. The focal depth of the lens used, resolution, and sample rate of the camera will play the key role. The focal depth, resolution and sample rate in the tests, the results of which are depicted in Fig. 10, equaled to approx. 2 cm, 1024x1024 px, and 10^4 fps, respectively.

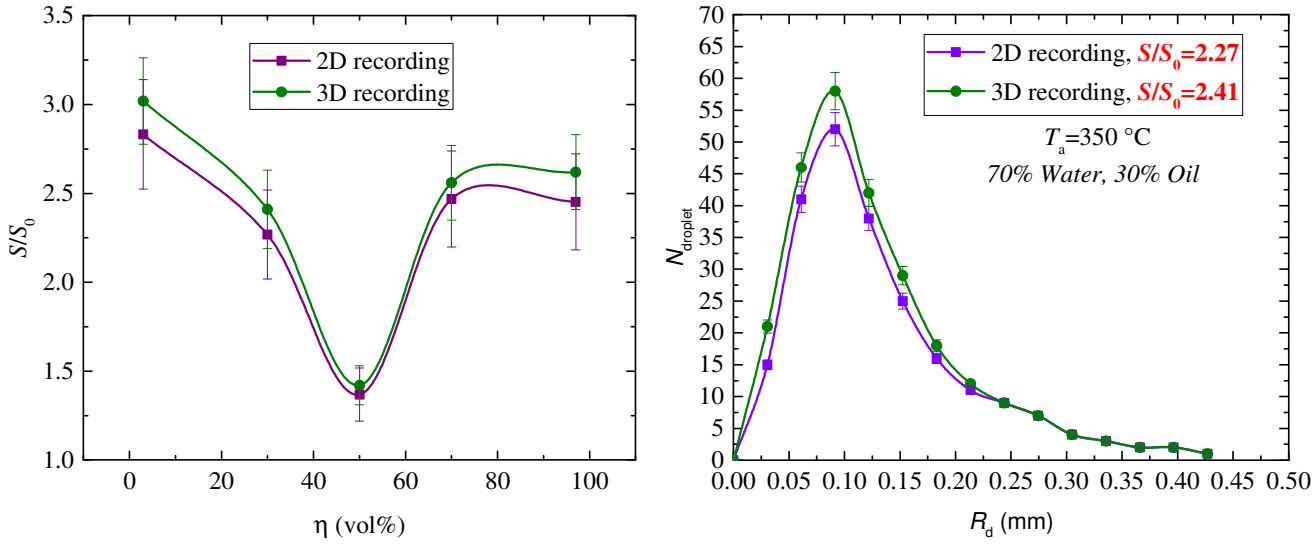

a *b*

Fig. 10. Results of the 2D and 3D recording of the breakup outcomes of the 15 µl-two-component droplets: *a* – ratio between the evaporation surface areas before and after breakup versus oil concentration; *b* – size distribution of child-droplets.

3.4. Impact on droplet heating and breakup

Preliminary analysis has shown that the paramount impact on two-component droplet heating and disintegration comes from a limited group of factors: concentration of components and heat flux supplied to the droplet surface (heating temperature). In the case of emulsion droplets, we need to add the following important factors [44, 45]: size of disperse phase droplets (water droplets in the volume of a flammable liquid, for instance, diesel), emulsion droplet size, water fraction in the emulsion, concentration and type of stabilizer. In order to explore the role of the main factors, we performed experiments with varying air flow temperature and velocity (by changing the convective heat flux), temperature in the muffle furnace (by changing the radiative heat flux), as well as the concentration and type of the liquid flammable component. The results are shown in Figs. 11–16.

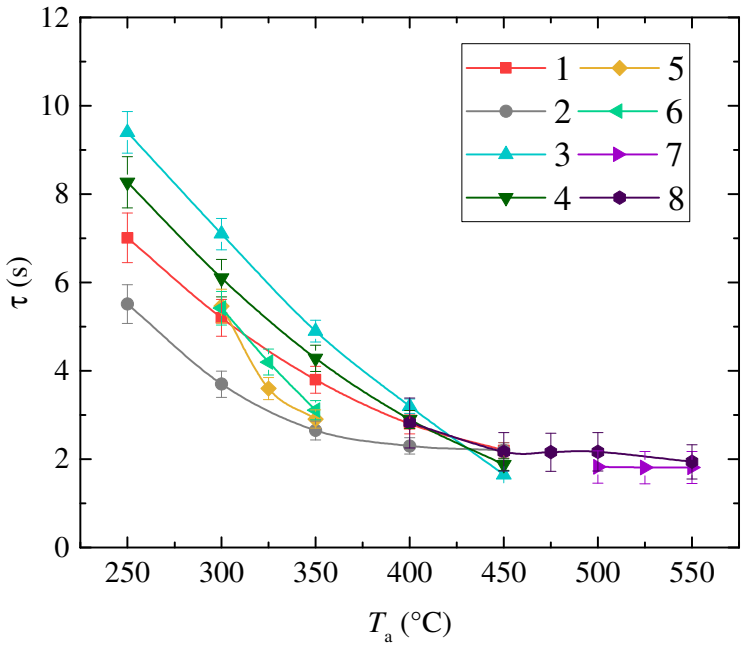

Fig. 11. Heating times before explosive breakup of droplets versus gaseous medium temperature (V_d=15 µl, U_a=2 m/s): 1 – 97 vol% water, 3 vol% petroleum; 2 – 95 vol% water, 5 vol% petroleum; 3 – 97 vol% water, 3 vol% oil; 4 – 95 vol% water, 5 vol% oil; 5 – 97 vol% water, 3 vol% gasoline; 6 – 95 vol% water, 5 vol% gasoline; 7 – 97 vol% water, 3 vol% kerosene; 8 – 95 vol% water, 5 vol% kerosene.

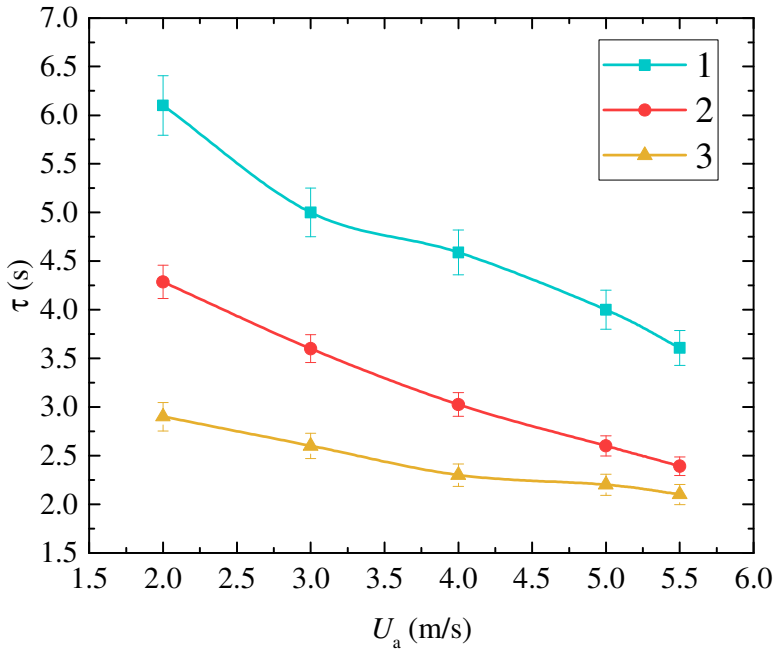

Fig. 12. Heating times before destruction of two-component droplets (V_d=15 µl) versus gas flow velocity: *1* – 95 vol% water, 5 vol% oil at T_a=300 °C; *2* – 95 vol% water, 5 vol% oil at T_a=350 °C; *3* – 95 vol% water, 5 vol% oil at T_a=400 °C.

Droplet lifetimes before puffing and micro-explosion decrease non-linearly with growing temperature and velocity of the incoming air flow (Figs. 11, 12), as well as the temperature in the muffle furnace (Fig. 13). This is conditioned largely by the non-linear (exponential) temperature dependences of

evaporation rates of flammable and non-flammable liquid components [1, 33, 34]. At the same time, the more significant the changes in these velocities with growing temperature and the lower the fuel component boiling, ignition and flash temperature, the more significantly the times τ changed. In some cases, it was difficult to record the droplet puffing due to a significant transformation of droplet surface while moving to the channel with heated air as well as droplets breaking away from the holder. Therefore, the plots are not obtained within the temperature range of 250 to 550 °C for all compositions.

The disintegration times of two-component droplets in the experiments with an incoming heated air (Figs. 11, 12) are several times shorter than in the experiments with the muffle furnace (Fig. 13) at identical temperatures. This is because at such mild temperatures, the radiative heat flux from the muffle furnace walls is several times lower than the convective heat flux from the air flow to the droplet surface. In particular, study [41] shows that a radiative heat flux will start dominating the convective one at temperatures above 800 °C. In this research, we did not explore such high temperatures, since it took several seconds for the explosive breakup of two-component droplets to occur at temperatures of 500 °C and above. A droplet is introduced by a moving robotic arm to the operating area of the channel for 0.5 s, but at high temperatures it is hard to provide even the motion of the object under study to the high-speed video recording area. At the same time, if we take into account the good repeatability of experimental times in Figs. 11, 13, it will be possible to use traditional extrapolation for the adequate assessment of the times τ for higher heating temperatures. The mechanism of the processes under study will remain the same.

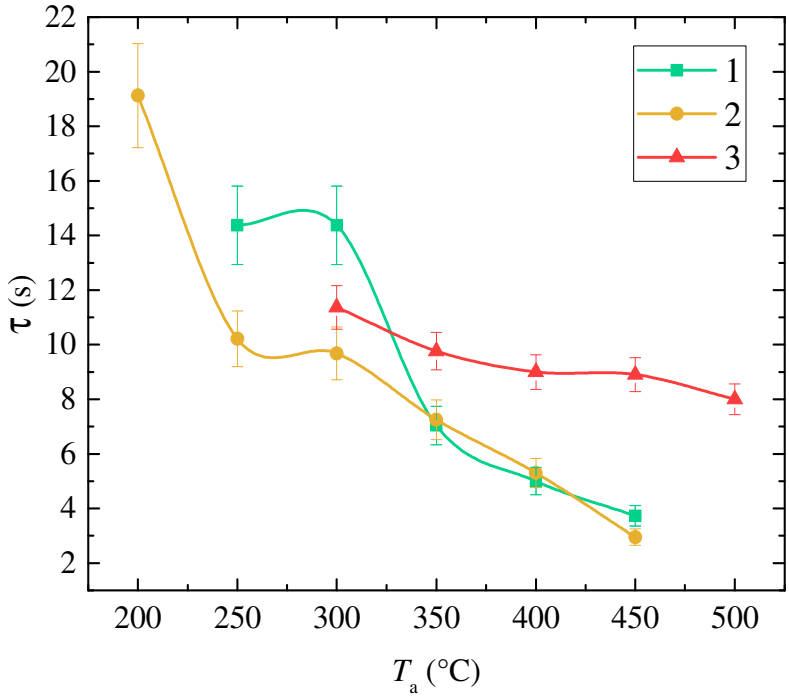

Fig. 13. Two-component droplet (V_d=15 μl) breakup time versus gaseous medium temperature at various heating temperatures: *1* – 30 vol% water, 70 vol% oil; *2* – 30 vol% water, 70 vol% diesel; *3* – 30 vol% water, 70 vol% solvent.

By varying the proportions of flammable and non-flammable components in a two-component liquid, we can increase or reduce the breakup time 3–4 times (Fig. 14) and sometimes even more (Fig. 15). Such patterns were observed in the experiments with a considerable convective heat flux towards the droplet surface. In a muffle furnace, changing the component concentration in a two-component droplet did not affect the breakup time much (Fig. 14). Most likely, when the radiative heat fluxes are at least as high as convective ones, the conditions shown by curves 2 and 3 in Fig. 14 will be repeated.

The non-monotonous nature of curve *1* in Fig. 14 illustrates the complicated mechanism of two-component droplet destruction in the heated air flow. It is safe to assume that the explosive breakup of such a droplet occurs if the sum of forces breaking up the droplet exceeds the sum of forces keeping its integrity. The former are the forces caused by the pressure of water vapors formed at a distance from the heated surface during the intense evaporation and boiling. This happens when fine droplets that are part of water-fuel emulsion are heated to high temperatures. As a result, the integrity of the near-surface layer of an emulsion droplet is disrupted, followed by a sharp decrease in its viscosity and shear strength. The forces destroying the droplet also include the friction shear stress of the air flowing around the droplet. Shear stress tears the near-surface layer of the droplet weakened by the rapid vaporization, intensifies the escape of water vapor bubbles into the ambient air and promotes the destruction of the initial droplet.

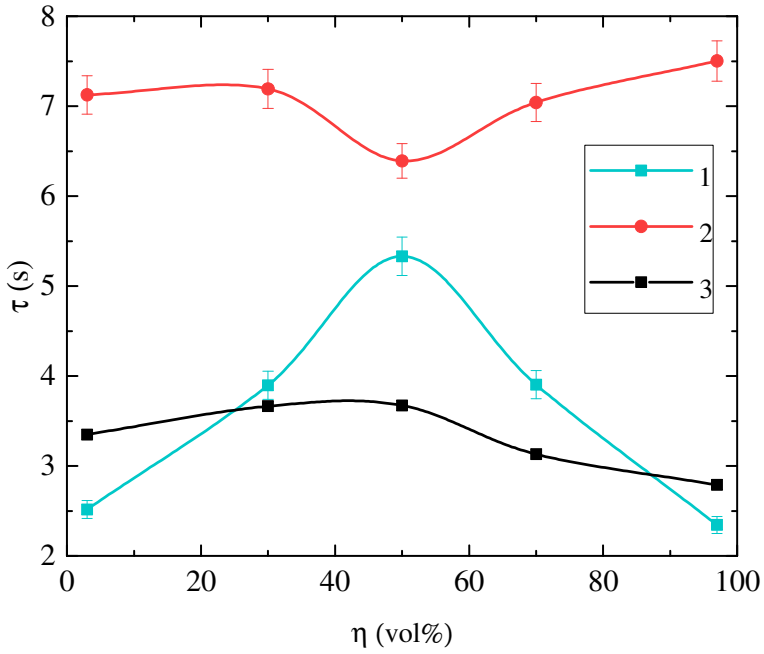

Fig. 14. Two-component droplet (V_d=15 µl) breakup time versus flammable liquid concentration (petroleum oil): *1* – convective heating at T_a=350 °C, U_a = 2 m/s; *2* – radiative heating at T_a=350 °C; *3* – radiative heating at T_a=500 °C.

An increase in the fraction of fuel (flammable component) in the emulsion or a two-component droplet within 50 vol% leads to another effect: growing viscosity and durability of the near-surface layer

of the initial droplet. This reinforcement of the near-surface layer of the emulsion or a two-component droplet increases its heating time to destruction (Fig. 14).

However, an increase in the fraction of the flammable component in an emulsion or two-component droplet does not only strengthen the droplet but also reduces its heat capacity. The smaller the share of water in a droplet, the lower the heat capacity and the faster the droplet will reach the water boiling temperature at the *fuel / water* interface. When that happens, the interface transforms significantly leading to droplet disintegration. With low water concentration in a droplet, water vapor can be heated to threshold temperatures corresponding to the high pressures in vapor bubbles. In this case, the breakup of the near-surface layer of an emulsion or two-component droplet occurs at higher temperatures than with low fuel concentration. The first portion of curve *1* in Fig. 14 corresponds to the conditions of such droplet destruction. Under radiative droplet heating, without a directed hot air flow, there is no stress at the droplet surface even at low velocities (Fig. 14), and the time of its destruction is much longer.

The experimentally established patterns in the heating and explosive breakup of droplets of two immiscible fluids with different component concentrations show that the breakup can be used successfully in a wide range of technologies and heating conditions. At the same time, varying the temperatures and concentrations makes it possible to increase and reduce the times τ several-fold. This result is the most valuable in this research, since it shows the allowable ranges of parameter variation and the best specifications of the corresponding thermal treatment or combustion chambers as well as their injection systems. It is important to provide a staged consecutive droplet breakup in the course of heating and evaporation. These patterns should be taken into account when designing thermal chambers and developing the regulations for the corresponding technologies.

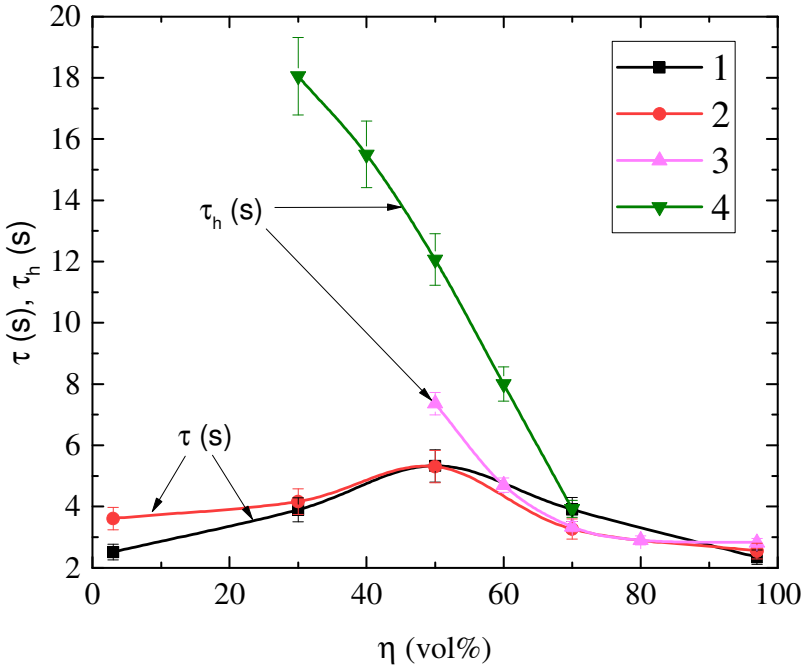

Fig. 15. Lifetime and breakup time of heterogeneous droplets (V_d=15 μl) versus flammable liquid concentration when type and properties of the components are varied: *1* – water–oil at T_a=350 °C, U_a=2

m/s; *2* – water–diesel fuel at T_a=350 °C, U_a=2 m/s; *3* – water–solvent at T_a=350 °C, U_a=2 m/s; *4* – water–diesel fuel (W/D emulsion) at T_a=350 °C, U_a=2 m/s.

In Fig. 15, a curve for two-component droplets with a solvent is plotted for η=50 vol%. At lower solvent concentrations, a two-component droplet did not break up but fell off the holder. This effect characterizes rather a weak molecular bond of the solvent and water. Therefore, we can provide the stable explosive breakup for them only with high concentrations of the liquid flammable component in two-component droplets. To compare the experimental results for W/D emulsion and two-component droplets, we present in Fig. 15 an additional curve of the lifetimes τ_h of W/D emulsion droplets versus the concentration of the flammable liquid. Unlike two-component droplets, the lifetime τ_h was recorded in the course of experiments, since no droplet explosion was observed. In the experiments with low flammable liquid concentrations (30 vol%), we could consistently observe evaporation. The concentration of 50 vol% provided both the evaporation and puffing (the probability of each of the two outcomes was about 50 %). With the 70 vol% concentration, we could only observe puffing. Dispersion was characterized by breaking away the parts of the W/D emulsion droplet.

The lifetimes and destruction times of heterogeneous droplets do not only depend on the above parameters but also on droplet dimensions. Fig. 16 shows the curve of W/D emulsion droplet lifetime versus droplet dimensions (radii). The radius of heterogeneous droplets ranged from 0.46 mm to 1 mm. The upper threshold of this range was based on the opportunity to fix a droplet on the holder. Larger droplets fell off before they reached the high-temperature gas area. The lower threshold of τ_h corresponds to the limitations of the equipment used.

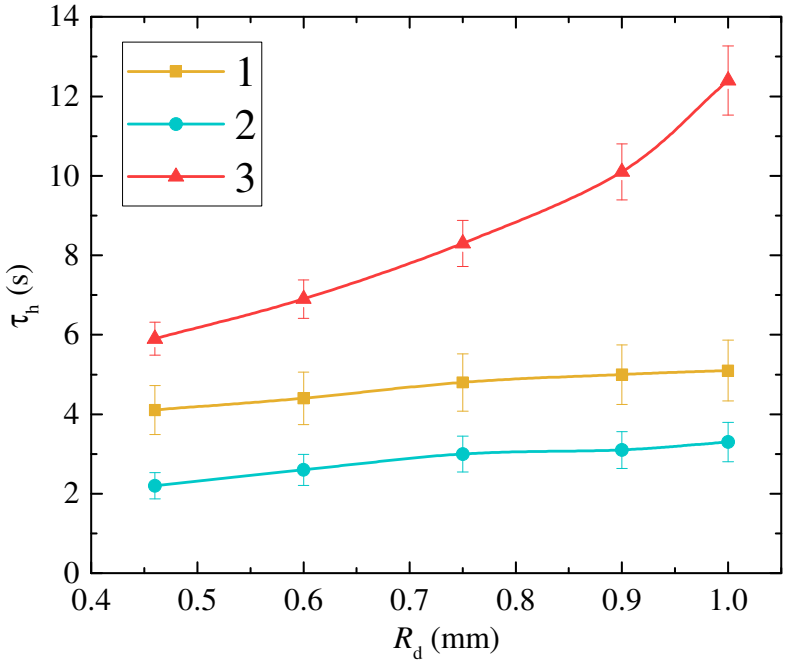

Fig. 16. W/D emulsion droplet lifetime versus initial droplet size (radius): *1* – 30 vol% water, 70 vol% diesel fuel at T_a = 350 °C, U_a = 2 m/s; *2* – 30 vol% water, 70 vol% diesel fuel at T_a=300 °C, U_a=2 m/s; *3* – 30 vol% water, 70 vol% diesel fuel at T_a=400 °C, U_a=2 m/s.

The experimental data, curves and approximation equations obtained in this research can help control the explosive breakup of droplets containing several liquid components with fundamentally different properties. The findings of this study can thus be applied not only for the development of the theory of two-phase and multi-component flows. They also push forward two sets of technologies: combustion of liquid and slurry fuels as well as thermal and flame liquid treatment. The conclusions from research [33] confirmed good prospects of a cost reduction for the ignition of fuels and an increase in the fullness of their burnout due to the breakup of droplets and particles in the fuels. In particular, 2–3-fold droplet and particle size reduction decreased the temperature by 60–110 °C and shortened the ignition delay times by 40–70 vol% (sometimes even more than twice). The adequate further local adjustment of the corresponding process units can significantly improve the efficiency of evaporation, ignition and burnout of fuels with different dispersion of the injected droplet aerosol. The main drawback of the modern thermal liquid treatment systems is that the unspecified impurities do not evaporate completely within one cycle, so the cycles have to be repeated. However, this drawback can be minimized in a staged way and overall eliminated, because the short-term explosive breakup of droplets into micron-sized fractions promotes its rapid evaporation and, as a result, volatilization or combustion of additives. The estimations show that an increase in the droplet heating and evaporation rate through their breakup provides the complete evaporation of the resulting droplet aerosol within 2–3 seconds. This time is enough for the evaporation or combustion of additives in one cycle of liquid treatment, since the dimensions of typical treatment chambers range from 3–5 to 7–8 m [46, 47] and the liquids remain there for treatment for up to 4–5 s [46, 47].

Study [32] for the first time presented the comparison results of the characteristics for the secondary atomization of droplets when using the two schemes: breakup due to micro-explosion and collision of the primary droplets when spraying at different angles. The breakup due to micro-explosion enableed to increase the S/S_0 ratio by 5-6 times. The study showed that depending on the state of the heterogeneous droplets, *i.e.* the droplets of two immiscible fluids and the emulsion droplets, the ranges of S/S_0 variation can be quite wide. The prospects of using the secondary atomization of droplets due to their micro-explosion were demonstrated clearly. In contrast to the droplets collision scheme, there is no necessity to modify combustion chambers or fuel supply and spray systems. It is necessary to provide for the certain temperature regime and the initial droplet sizes. Based on the research findings, it is possible to coordinate the temperature regimes, sizes of droplets, and their compositions and in such a manner to meet the conditions for the sustainable breakup of droplets with the attainment of the required values of S/S_0.

4. Conclusions

(i) The experiments identified the conditions for the four possible outcomes of two-component droplet heating. In particular, at the air temperature of up to 150–200 °C, a two-phase droplet falls off the holder, at 200 °C to 250 °C, small fragments broke away from the droplet surface, at 300 °C to 350 °C, a droplet broke up into relatively large fragments (sized up to 30–40 % of the initial heated droplet), and at over 400 °C, a droplet underwent an explosive breakup to form an aerosol.

(ii) Among the differences between the threshold puffing conditions for droplets of two immiscible fluids and W/D emulsions is that two-component droplets puffed at 200 °C and emulsion droplets, at over 350 °C.

(iii) The video frame analysis shows that the breakup of a single droplet yields 5 to 20 large liquid fragments or even an aerosol with more than 200–300 droplets sized 0.01 mm. At the same time, the faster the breakup process, the more droplets are formed in a fuel aerosol.

(iv) Of the factors under study, the temperature of the heating medium and component concentrations have the greatest impact on the final characteristics of heterogeneous droplet destruction. For instance, if the temperature increases from 250 °C to 550 °C, the explosive breakup time is reduced 3–7 times and droplet size in the resulting aerosol goes down 80–90 %. If the proportion of water goes up from 3 vol% to 50 vol%, the explosive breakup time increases 2–5-fold and the droplet size in the resulting aerosol grows by 30–40 %.

(v) The most ineffective proportion of components in two-component droplets and W/D emulsion droplets is 50 vol% of flammable liquid and 50 vol% of water. The greatest breakup performance is achieved if adding no more than 3 vol% of water to a droplet of flammable liquid or fuel. In this case, breakup almost instantaneously results in the formation of a fine aerosol and a gas-vapor cloud.

Acknowledgments

Research was funded by Russian Science Foundation (project 18–71–10002). The authors are grateful to the team of *SpecChemTechnology* (http://schemtec.ru/) and personally to *Vyacheslav Yanovsky* for their help in the preparation of fuel emulsions and analysis of their properties.

Nomenclature

n – number of droplets;

Q_c – heat of combustion, MJ/kg;

Q_v – heat of vaporization, MJ/kg;

R_d – droplet radius, mm;

R_{d0} – initial droplet radius, mm;

R_{d1} – droplet radius at the moment t, mm;

R_{dn} – mean size of droplets in a group, mm;

S – total area of the liquid evaporation surface, mm^2;

S_0 – initial droplet surface area, mm^2;

S_1 – droplet surface area at the moment t, mm^2;

S_m – frontal cross-sectional area of a droplet, mm^2;

t – time, s;

T_a – gas flow temperature, °C;

T_b – boiling temperature, °C;

T_d – temperature in the water droplet, °C

T_f – flash temperature, °C;

T_i – ignition temperature, °C;

U_a – high-temperature gas flow velocity, m/s;

V_d – droplet volume, µl.

Greek

α – luminous intensity, brightness units;

η – flammable liquid concentration, vol%;

µ – dynamic viscosity, Pa·s;

ρ – density, kg/m^3;

σ – surface tension, 10^{-3} N/m;

τ – heterogeneous droplet breakup times, s;

τ_h – heterogeneous droplet lifetimes, s.

References

1. S.S. Sazhin, Modelling of fuel droplet heating and evaporation: Recent results and unsolved problems, Fuel. 196 (2010) 69-101. https://doi.org/10.1016/j.fuel.2017.01.048.
2. S.A. Kalogirou, Seawater desalination using renewable energy sources, Prog. Energy Combust. Sci. 31 (2005) 242–281. https://doi.org/10.1016/j.pecs.2005.03.001.
3. M.A. Shannon, P.W. Bohn, M. Elimelech, J.G. Georgiadis, B.J. Mariñas, A.M. Mayes, Science and technology for water purification in the coming decades, Nature. 452 (2008) 301–310. https://doi.org/10.1038/nature06599.
4. R.J. Romero, A. Rodríguez-Martínez, Optimal water purification using low grade waste heat in an absorption heat transformer, Desalination. 220 (1–3) (2008) 506–513. https://doi.org/10.1016/j.desal.2007.05.026.
5. P.A. Strizhak, R.S. Volkov, The integral characteristics of the deceleration and entrainment of water droplets by the counter flow of high-temperature combustion products, Exp. Therm. Fluid Sci. 75 (2016) 54–65. https://doi.org/10.1016/j.expthermflusci.2016.01.018.
6. R.S. Volkov, P.A. Strizhak, Motion of water droplets in the counter flow of high-temperature combustion products, Heat Mass Transfer. 54 (2017) 1–15. https://doi.org/10.1007/s0023.

7. G.V. Kuznetsov, M.V. Piskunov, P.A. Strizhak, How to improve efficiency of using water when extinguishing fires through the explosive breakup of drops in a flame: Laboratory and field tests, Int. J. Therm. Sci. 121 (2017) 398–409. https://doi.org/10.1016/j.ijthermalsci.2017.08.004.
8. Y. Suzuki, T. Harada, H. Watanabe, M. Shoji, Y. Matsushita, H. Aoki, T. Miura, Visualization of aggregation process of dispersed water droplets and the effect of aggregation on secondary atomization of emulsified fuel droplets, Proc. Combust. Inst. 33 (2011) 2063–2070. https://doi.org/10.1016/j.proci.2010.05.115.
9. D. Tarlet, C. Josset, J. Bellettre, Comparison between unique and coalesced water drops in micro-explosions scanned by differential calorimetry, Int. J. Heat and Mass Transfer. 95 (2016) 689–692. https://doi.org/10.1016/j.ijheatmasstransfer.2015.12.054.
10. H. Watanabe, T. Harada, Y. Matsushita, H. Aoki, T. Miura, The characteristics of puffing of the carbonated emulsified fuel, Int. J. Heat Mass Transfer. 52 (2009) 3676–3684. https://doi.org/10.1016/j.ijheatmasstransfer.2009.02.033.
11. Z. Yin, P. Nau, W. Meier, Responses of combustor surface temperature to flame shape transitions in a turbulent bi-stable swirl flame, Exp. Therm Fluid Sci. 82 (2017) 50–57. https://doi.org/10.1016/j.expthermflusci.2016.11.004.
12. P. Nau, P. Kutne, G. Eckel, W. Meier, C. Hotz, S. Fleck, Infrared absorption spectrometer for the determination of temperature and species profiles in an entrained flow gasifier, Appl. Optics. 56 (2017) 2982–2990. https://doi.org/10.1364/AO.56.002982.
13. K. Warncke, S. Gepperth, B. Sauer, A. Sadiki, J. Janicka, R. Koch, H.-J. Bauer, Experimental and numerical investigation of the primary breakup of an airblasted liquid sheet, Int. J. Multiphase Flow. 91 (2017) 208–224. https://doi.org/10.1016/j.ijmultiphaseflow.2016.12.010.
14. D. Tarlet, C. Allouis, J. Bellettre, The balance between surface and kinetic energies within an optimal micro-explosion, Int. J. Therm. Sci. 107 (2016) 179–183. https://doi.org/ 10.1016/j.ijthermalsci.2016.04.008.
15. D. Tarlet, E. Mura, C. Josset, J. Bellettre, C. Allouis, P. Massoli, Distribution of thermal energy of child-droplets issued from an optimal micro-explosion, Int. J. of Heat and Mass Transfer. 77 (2014) 1043–1054. https://doi.org/10.1016/j.ijfiheatmasstransfer.2014.06.054.
16. A.V. Kim, N.N. Medvedev, A. Geiger, Molecular dynamics study of the volumetric and hydrophobic properties of the amphiphilic molecule C_8E_6, J. Mol. Liq. Spec. 189 (2014) 74–80. https://doi.org/10.1016/j.molliq.2013.05.001.
17. V.P. Voloshin, A.V. Kim, N.N. Medvedev, R. Winter, A. Geiger, Calculation of the volumetric characteristics of biomacromolecules in solution by the Voronoi-Delaunay technique, Biophys. Chem. 192 (2014) 1–9. https://doi.org/10.1016/j.bpc.2014.05.001.
18. G.V. Kuznetsov, M.V. Piskunov, P.A. Strizhak, Evaporation, boiling and explosive breakup of heterogeneous droplet in a high-temperature gas, Int. J. Heat Mass Transfer. 92 (2016) 360–369.

https://doi.org/10.1016/j.ijheatmasstransfer.2015.08.061.

19. O.V. Vysokomornaya, M.V. Piskunov, P.A. Strizhak, Breakup of heterogeneous water drop immersed in high-temperature air, Appl. Therm. Eng. 127 (2017) 1340–1345. https://doi.org/10.1016/j.applthermaleng.2017.08.162.
20. P.A. Strizhak, M.V. Piskunov, R.S. Volkov, J.C. Legros, Evaporation, boiling and explosive breakup of oil-water emulsion drops under intense radiant heating, Chem. Eng. Res. Des. 127 (2017) 72–80. https://doi.org/10.1016/j.cherd.2017.09.008.
21. M.V. Piskunov, P.A. Strizhak, Using planar laser-induced fluorescence to explain the mechanism of heterogeneous water droplet boiling and explosive breakup, Exp. Therm Fluid Sci. 91 (2018) 103–116. https://doi.org/10.1016/j.expthermflusci.2017.10.018.
22. P. Lavieille, F. Lemoine, G. Lavergne, J.F. Virepinte, M. Lebouche, Temperature measurements on droplets in monodisperse stream using laser-induced fluorescence, Exp. Fluids. 29 (2000) 429-437. https://doi.org/10.1007/s003480000.
23. G. Castanet, A. Labergue, F. Lemoine, Internal temperature distributions of interacting and vaporizing droplets, Int. J. Therm. Sci. 50 (2011) 1181-1190. https://doi.org/10.1016/j.ijthermalsci.2011.02.001.
24. G. Castanet, L. Perrin, O. Caballina, F. Lemoine, Evaporation of closely-spaced interacting droplets arranged in a single row, Int. J. Heat and Mass Transfer. 93 (2016) 788-802. https://doi.org/10.1016/j.ijheatmasstransfer.2015.09.064.
25. F. Lemoine, G. Castanet, Temperature and chemical composition of droplets by optical measurement techniques: A state-of-the-art review, Exp. Fluids. 54 (2013). https://doi.org/10.1007/s00348-013-1572-9.
26. Y.K. Akhmetbekov, S.V. Alekseenko, V.M. Dulin, D.M. Markovich, K.S. Pervunin, Planar fluorescence for round bubble imaging and its application for the study of an axisymmetric two-phase jet, Exp. Fluids. 48 (2010) 615–629. https://doi.org/10.1007/s00348-009-0797-0.
27. C. Abram, B. Fond, A.L. Heyes, F. Beyrau, High-speed planar thermometry and velocimetry using thermographic phosphor particles, Appl. Phys. B. 111 (2013) 155–160. https://doi.org/10.1007/s00340-013-5411-8.
28. A.S. Nebuchinov, Y.A. Lozhkin, A.V. Bilsky, D.M. Markovich, Combination of PIV and PLIF methods to study convective heat transfer in an impinging jet, Exp. Therm. Fluid Sci. 80 (2017) 139–146. https://doi.org/10.1016/j.expthermflusci.2016.08.009.
29. G.V. Kuznetsov, P.A. Strizhak, R.S. Volkov, O.V. Vysokomornaya, Integral characteristics of water droplet evaporation in high temperature combustion products of typical flammable liquids using SP and IPI methods, Int. J. Therm. Sci. 108 (2016) 218–234. https://doi.org/10.1016/j.ijthermalsci.2016.05.019.

30. R.S. Volkov, P.A. Strizhak, Using Planar Laser Induced Fluorescence to explore the mechanism of the explosive disintegration of water emulsion droplets exposed to intense heating, Int. J. of Therm. Sci. 127 (2018) 126–141. https://doi.org/10.1016/j.ijthermalsci.2018.01.027.
31. D.V. Antonov, R.S. Volkov, P.A. Strizhak, An explosive disintegration of heated fuel droplets with adding water, Chem. Eng. Res. Des. 140 (2018) 292–307. https://doi.org/10.1016/j.cherd.2018.10.031.
32. D. Antonov, J. Bellettre, D. Tarlet, P. Massoli, O. Vysokomornaya, M. Piskunov, Impact of Holder Materials on the Heating and Explosive Breakup of Two-Component Droplets, Energies. 11 (2018) 1–17. https://doi.org/10.3390/en11123307.
33. D.O. Glushkov, P.A. Strizhak, M.Yu. Chernetskii, Organic Coal-Water Fuel: Problems and Advances (Review), Therm. Eng. 63 (2016) 707–717. https://doi.org/10.1134/S0040601516100037.
34. D.O. Glushkov, S.Yu. Lyrschikov, S.A. Shevyrev, P.A. Strizhak, Burning Properties of Slurry Based on Coal and Oil Processing Waste, Energy Fuels. 30 (2016) 3441–3450. https://doi.org/10.1021/acs.energyfuels.5b02881.
35. V.A. Yanovsky, M.O. Andropov, R.S. Fakhrislamova, R.A. Churkin, K.M. Minaev, O.S. Ulyanova, Rheological properties of inverse emulsions stabilized by ethanolamides of tall oil fatty acids, MATEC Web. Conf., 85 (2016) 1–7. https://doi.org/10.1051/matecconf/20168501020.
36. K. Minaev, A. Epikhin, D. Novoseltsev, M. Andropov, V. Yanovsky, O. Ulyanova, Research of inverted emulsions properties on the base of new emulsifiers, IOP Conf. Ser. Earth Environ, 21 (2014) 1–6.
37. M.Y. Khan, Z.A.A. Karim, A.R.A. Aziz, M.R. Heikal, C. Crua, Puffing and Microexplosion Behavior of Water in Pure Diesel Emulsion Droplets During Leidenfrost Effect, Combust. Sci. Technol. 189 (2017) 1186–1197. https://doi.org/10.1080/00102202.2016.1275593.
38. P.A. Strizhak, R.S. Volkov, G. Castanet, F. Lemoine, O. Rybdylova, S.S. Sazhin, Heating and evaporation of suspended water droplets: experimental studies and modelling, Int. J. Heat and Mass Transfer. 127 (2018) 92–106. https://doi.org/10.1016/j.ijheatmasstransfer.2018.06.103.
39. E. Mura, P. Massoli, C. Josset, K. Loubar, J. Bellettre, Study of the micro-explosion temperature of water in oil emulsion droplets during the Leidenfrost effect, Exp. Therm Fluid Sci. 43 (2012) 63–70. https://doi.org/10.1016/j.expthermflusci.2012.03.027.
40. E. Mura, C. Josset, K. Loubar, G. Huchet, J. Bellettre, Effect of dispersed water droplet size in microexplosion phenomenon for water in oil emulsion, Atomization Sprays. 20 (2010) 791–799. https://doi.org/10.1615/AtomizSpr.v20.i9.40.
41. G.V. Kuznetsov, M.V. Piskunov, R.S. Volkov, P.A. Strizhak, Unsteady temperature fields of evaporating water droplets exposed to conductive, convective and radiative heating, Appl. Therm. Eng. 131 (2018) 340–355. https://doi.org/10.1016/j.applthermaleng.2017.12.021.

42. R.S. Volkov, P.A. Strizhak, Measuring the temperature of a rapidly evaporating water droplet by Planar Laser Induced Fluorescence, Measurement. 135 (2019) 231–243. https://doi.org/10.1016/j.measurement.2018.11.047.
43. N.V. Bulanov, Explosive boiling of dispersed liquids, UrGUPS, 2011, p. 232.
44. A.M. Ithnin, H. Noge, H.A. Kadir, W. Jazair, An overview of utilizing water-in-diesel emulsion fuel in diesel engine and its potential research study, J. Energy Inst. 87 (2014) 273–288. https://doi.org/10.1016/j.joei.2014.04.002.
45. Y. Morozumi, Y. Saito, Effect of Physical Properties on Microexplosion Occurrence in Water-in-Oil Emulsion Droplets, Energy Fuels. 24 (2010) 1854–1859. https://doi.org/10.1021/ef9014026.
46. R.S. Volkov, A.O. Zhdanova, G.V. Kuznetsov, P.A. Strizhak, Experimentally Determining the Sizes of Water Flow Droplets Entrained by High Temperature Gases, Therm. Eng. 62 (2015) 586–592. https://doi.org/10.1134/S0040601515080091.
47. R.S. Volkov, G.V. Kuznetsov, P.A. Strizhak, Movement and Evaporation of Water Droplets under Conditions Typical for Heat-Exchange Chambers of Contact Water Heaters, Therm. Eng. 63 (2016) 666–673. https://doi.org/10.1134/S004060151609007X.

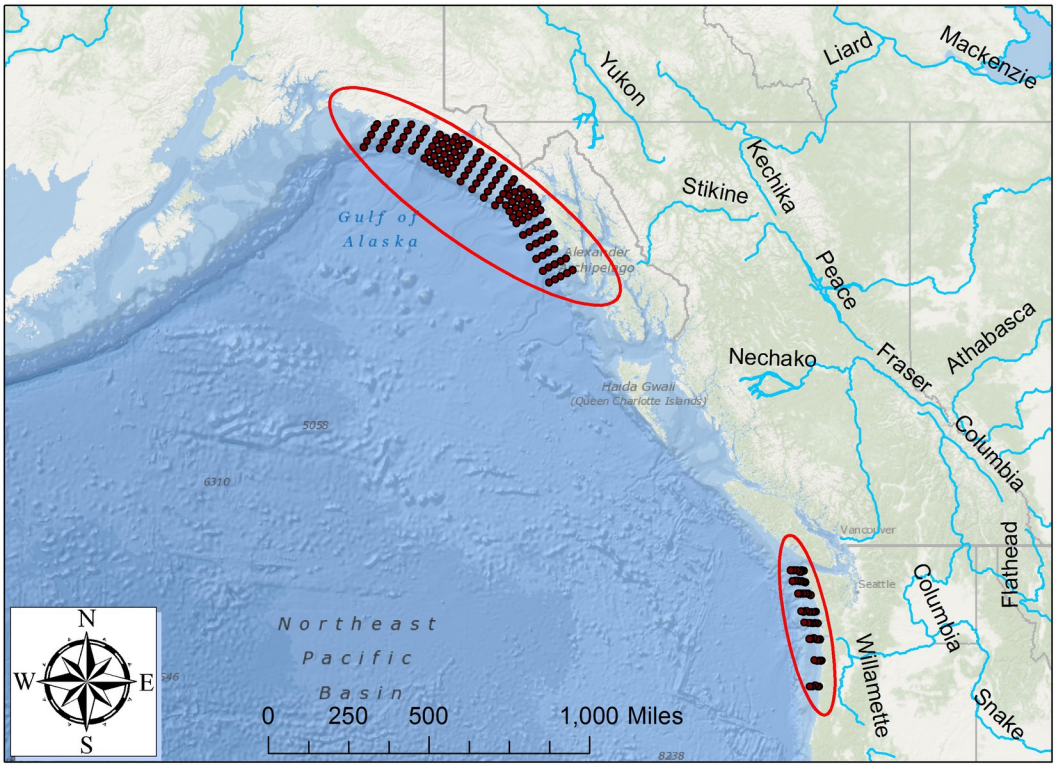
Yukon
Liard
Mackenzie
Kechika
Stikine
Peace
Nechako
Fraser
Athabasca
Columbia
Flathead
Columbia
Willamette
Snake
Gulf of Alaska
Alexander Archipelago
Haida Gwaii (Queen Charlotte Islands)
Vancouver
Seattle
Northeast Pacific Basin
5058
6310
8238
N
W
E
S
0 250 500 1,000 Miles

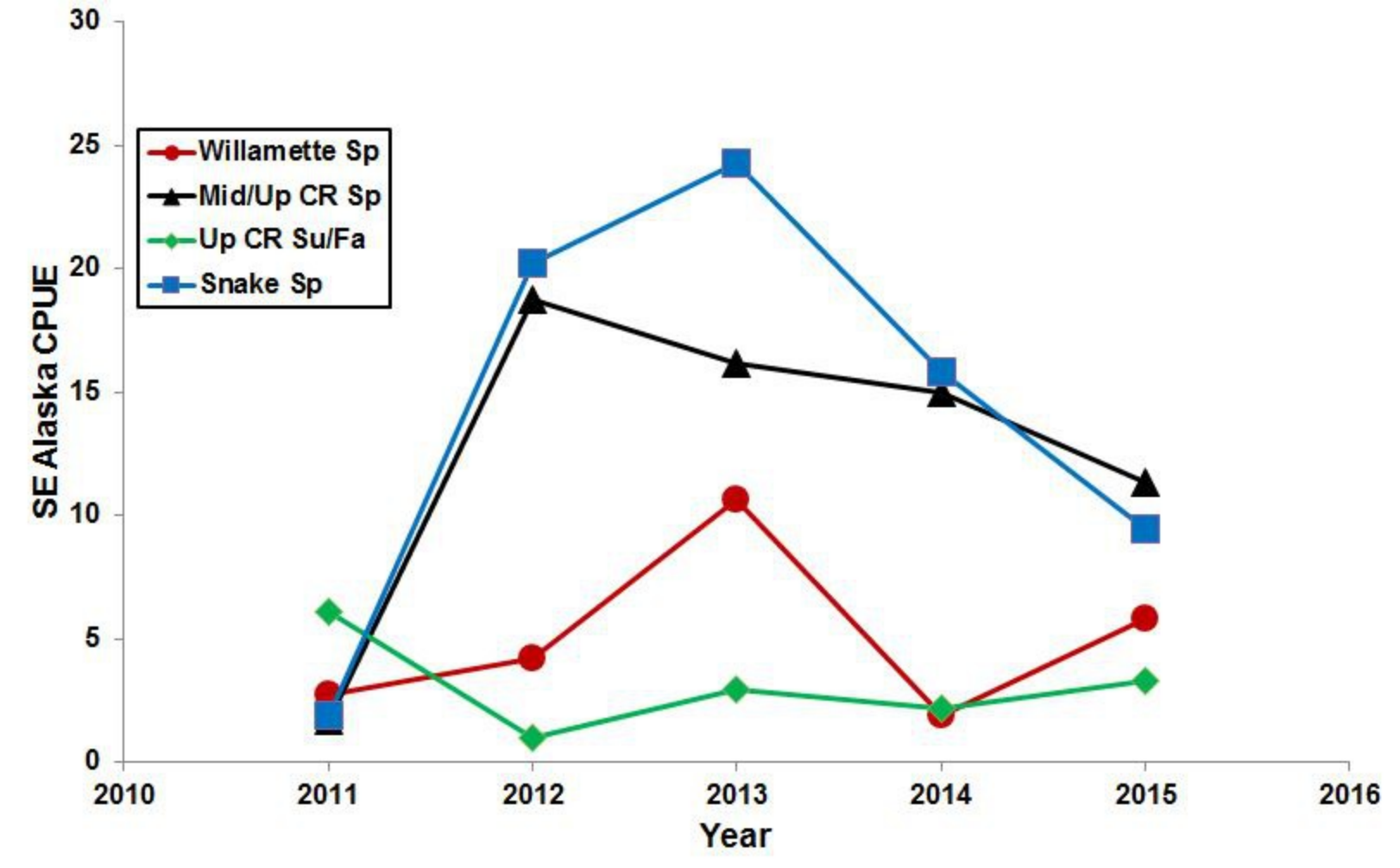
Willamette Sp
Mid/Up CR Sp
Up CR Su/Fa
Snake Sp
SE Alaska CPUE
Year
0
5
10
15
20
25
30
2010
2011
2012
2013
2014
2015
2016

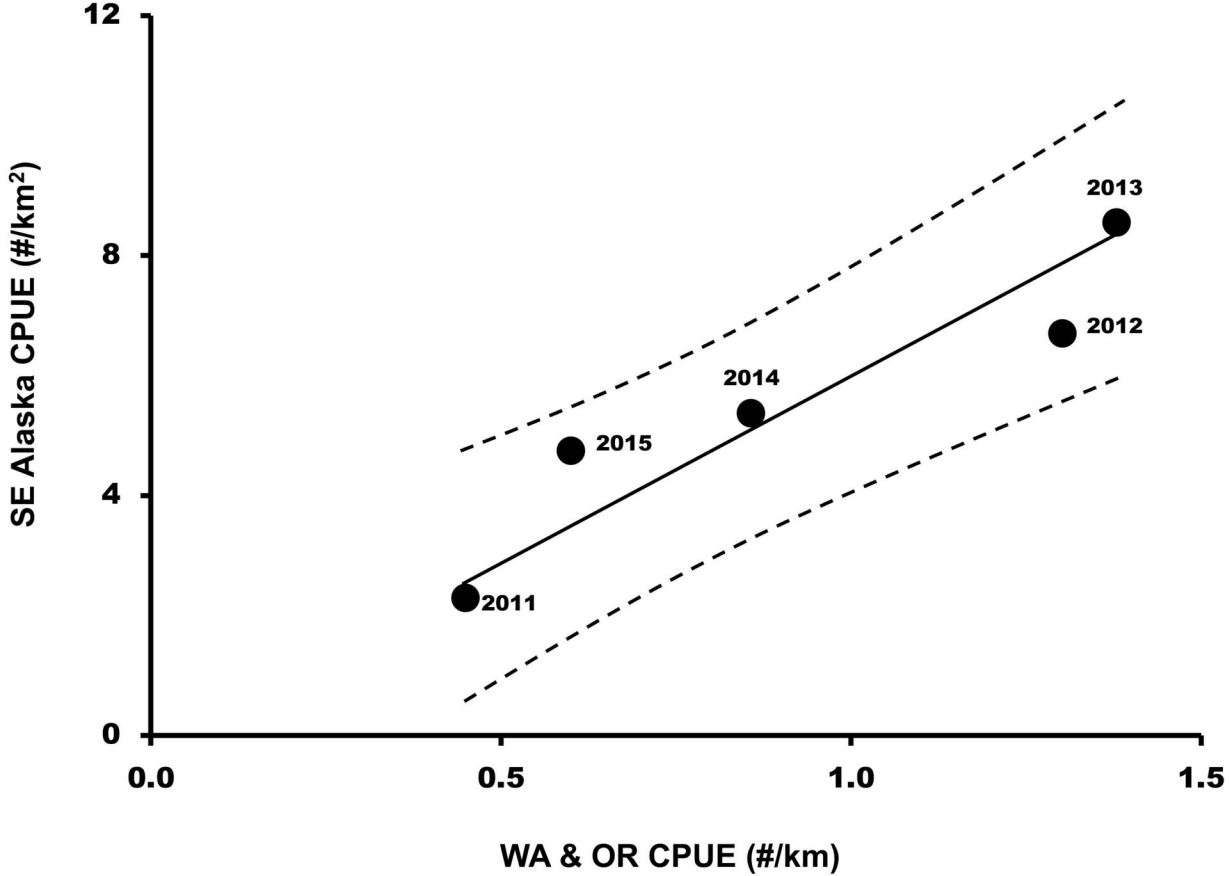
12
8
4
0
SE Alaska CPUE (#/km2)
0.0
0.5
1.0
1.5
WA & OR CPUE (#/km)
2013
2012
2014
2015
2011

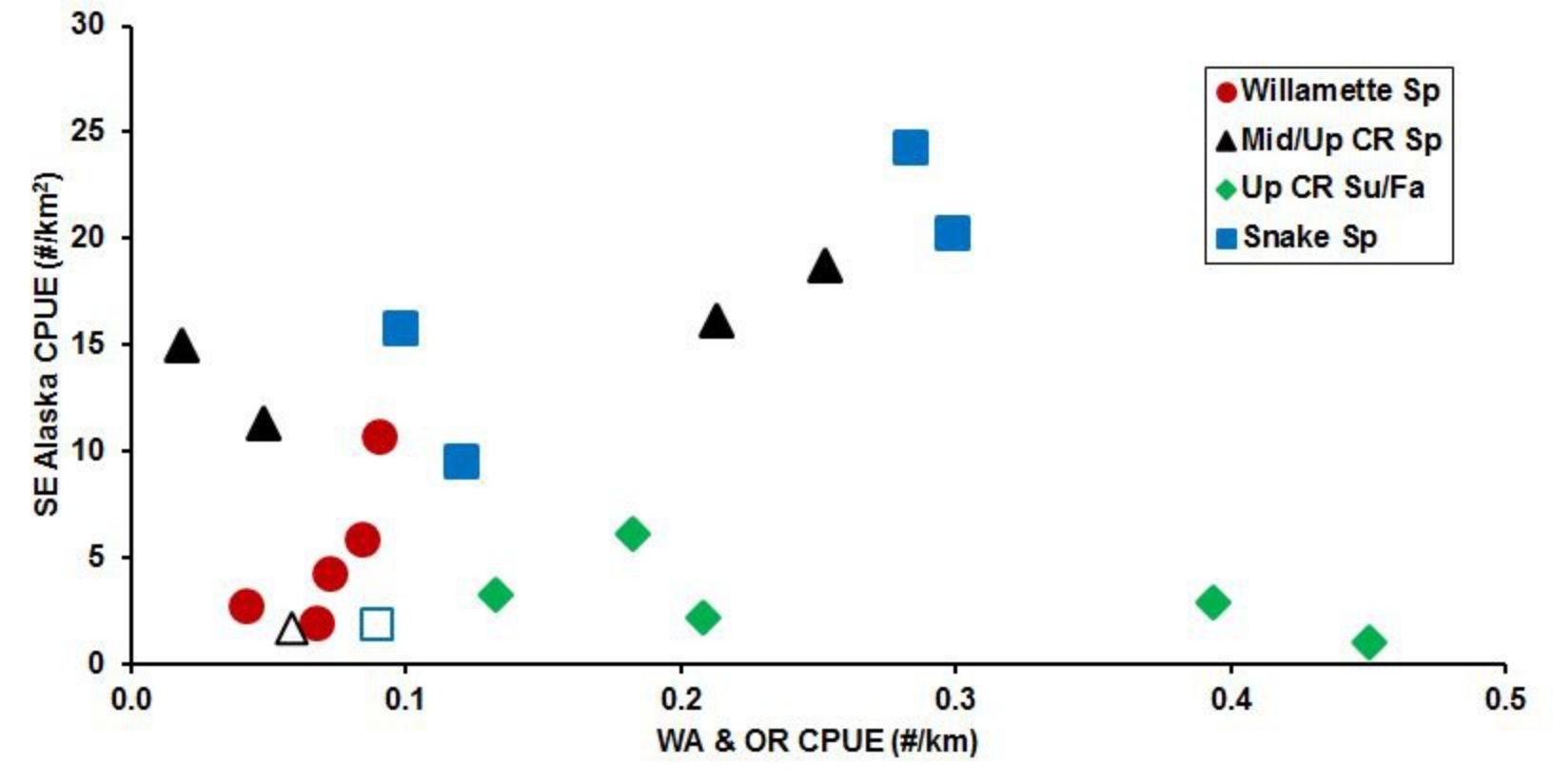
Willamette Sp
Mid/Up CR Sp
Up CR Su/Fa
Snake Sp
SE Alaska CPUE (#/km²)
WA & OR CPUE (#/km)
0
5
10
15
20
25
30
0.0
0.1
0.2
0.3
0.4
0.5

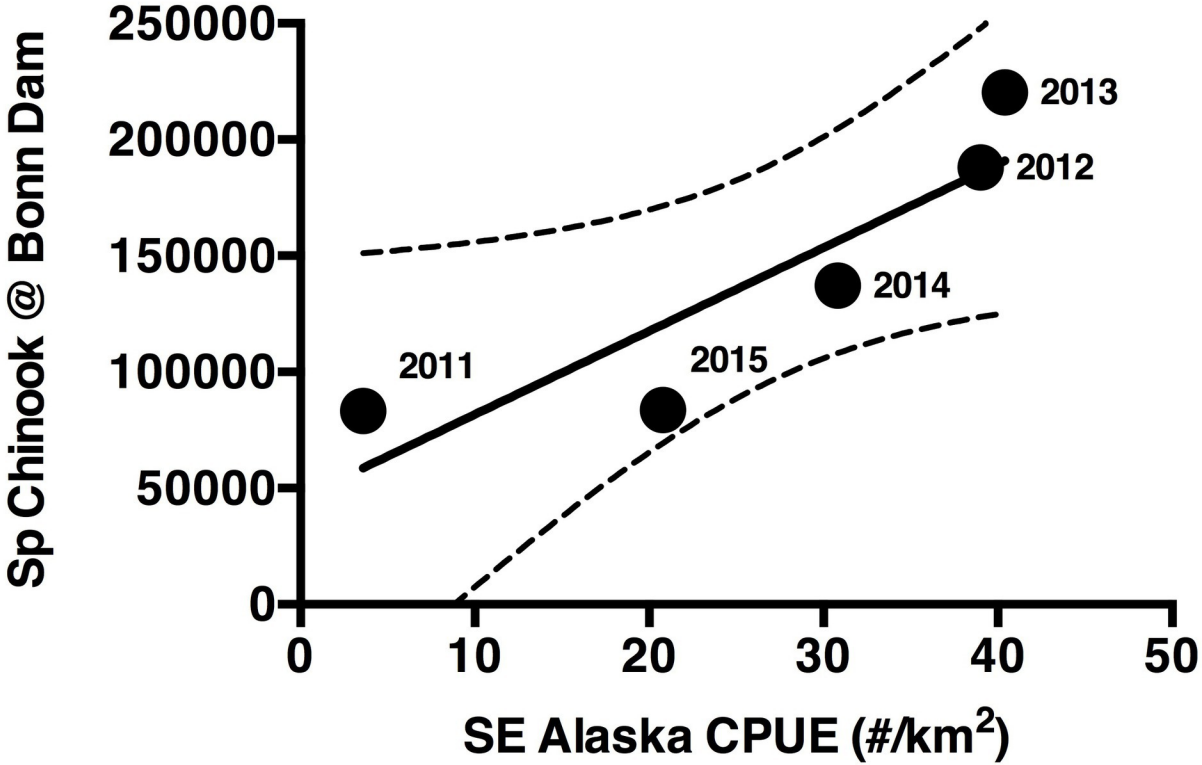
Sp Chinook @ Bonn Dam
250000
200000
150000
100000
50000
0
0
10
20
30
40
50
SE Alaska CPUE (#/km2)
2013
2012
2014
2011
2015